



## Trace-element geochemistry of diamondite: Crystallisation of diamond from kimberlite–carbonatite melts

Sonal Rege <sup>a,\*</sup>, W.L. Griffin <sup>a</sup>, G. Kurat <sup>b</sup>, S.E. Jackson <sup>a</sup>, N.J. Pearson <sup>a</sup>, Suzanne Y. O'Reilly <sup>a</sup>

<sup>a</sup> GEMOC ARC National Key Centre, Department of Earth and Planetary Sciences, Macquarie University, Sydney, NSW 2109, Australia

<sup>b</sup> Naturhistorisches Museum, Vienna, Austria

### ARTICLE INFO

#### Article history:

Received 24 April 2007

Accepted 7 June 2008

Available online 12 June 2008

#### Keywords:

Diamond trace elements

Diamondite

Mantle fluids

Kimberlite–carbonatite melts

LAM-ICPMS

### ABSTRACT

Quantitative trace-element analyses of 38 elements have been carried out in 11 samples of polycrystalline diamond (diamondite) from southern Africa by LAM-ICPMS. The samples are divided into “peridotitic” and “eclogitic” types based on the compositions of garnet and clinopyroxene intergrown with the diamond. The trace-element patterns of the diamondite samples reflect mixtures of diamond and submicroscopic inclusions of fluid±solid phases, and are interpreted as representing the fluids from which the diamondite crystallised. They are similar to parent-melt compositions calculated from macroscopic garnet and clinopyroxene inclusions in the diamondites, and suggest that the diamondites, like many fibrous diamonds, crystallised from melts in the kimberlite–carbonatite spectrum. Multi-element spikes seen in the time-resolved LAM-ICPMS analyses indicate the presence of several, probably submicroscopic, solid phases: garnet, clinopyroxene, an Y–Yb rich (fluoride?) phase, a sulfide rich in Cu–Pb–Zn–Co–Ni, a LIMA-type phase, a carbonate, ilmenite, chromite and mica. The similarity in trace-element patterns of the “peridotitic” and “eclogitic” diamondites suggests that both types have crystallised from the same type of metasomatic fluid. This fluid may have evolved from “peridotitic” to “eclogitic” by the removal of chromite±sulfide±ilmenite.

© 2008 Elsevier B.V. All rights reserved.

## 1. Introduction

Monocrystalline diamond is the form of diamond that is of most economic importance, and hence has been most studied in terms of origin and formation. However, diamond also occurs in many varieties of polycrystalline aggregate: boart, stewartite, framesite, hailstone boart, shot boart, ballas and carbonado (Orlov, 1977). All are believed to have crystallised under conditions of rapid growth, different from those that produced monocrystalline diamonds.

Diamondites are fine-grained (<100 µm) to coarse grained (>1 mm) rocks consisting almost entirely of polycrystalline diamond with abundant pores and cavities (Gurney and Boyd, 1982; Kirkley et al., 1994; Kurat and Dobosi, 2000; Dobosi and Kurat 2002, Jacob et al., 2000; Honda et al., 2004). They are distinguished from framesites, which have a finer grain size and a generally more compact structure. In some samples of diamondite, the diamond is intergrown with silicates (garnet and clinopyroxene) and with other minor phases such as chromite and ilmenite. Open cavities lined with euhedral diamonds imply the presence of fluids during crystallisation, and Kurat and Dobosi (2000) showed that silicates and diamonds very likely grew synchronously from the same fluid. They suggested that

these “polycrystalline diamonds” should be regarded as rocks, and therefore should be classified as diamond rocks or ‘diamondites’; this nomenclature has been followed here.

We have used laser-ablation microprobe-inductively coupled plasma mass spectrometry (LAM-ICPMS) techniques (Rege et al., 2005) to analyse the trace-element contents of eleven diamondite samples. The analysed trace elements are assumed to be present in the form of submicroscopic fluid/solid inclusions in the ‘diamond’ portion of the diamondites, representing the fluid/melt from which they have precipitated. The data provide insights into the composition of this parent fluid and help to understand the relationship between diamondites and the formation of monocrystalline and/or fibrous diamonds in the mantle.

## 2. Samples

The diamondite samples used for this study come from the larger set studied by Kurat and Dobosi (2000) and Dobosi and Kurat (2002). Although the exact locality for the samples is unknown, they are assumed (Kurat and Dobosi, 2000) to be from southern Africa, probably Botswana; as similar samples have been described from this area (Gurney and Boyd, 1982; Kirkley et al., 1994) and the large diamonds of hexahedral (‘cubic’) habit that were sold together with these diamondite samples are consistent with this origin.

The samples vary in colour from medium to dark grey, to almost black; individual diamond grains may range from white to dark gray.

\* Corresponding author.

E-mail address: [rege\\_sonal@yahoo.com](mailto:rege_sonal@yahoo.com) (S. Rege).

**Table 1**

Group averages and sample average values of the trace-element analyses of peridotitic and eclogitic diamondites (ppm)

Element	Peridotitic diamondites													P-D017
	P-D012													
No. of analyses	GP-1-Avg	GP-2-Avg	GP-3-Avg	GP-4-Avg	GP-5-Avg	GP-6-Avg	GP-7-Avg	GP-8-Avg	GP-9-Avg	GP-10-Avg	GP-11-Avg	P-D012-AVG	GP-1-Avg	
	4	6	3	3	2	3	7	3	2	4	5	42	2	
Na	45.0	5.55	1242	117	32.3	88.7	18.7	26.1	87.7	64.8	56.4	162	35.5	
Al	293	8.05	3476	367	189	431	311	203	446	427	310	587	500	
Ca	410	33.1	1770	275	112	1590	229	363	1359	600	659	673	467	
Mg	675	61.2	8075	929	272	1899	3613	528	2372	1205	1009	1876	7817	
Mn	8.64	0.60	9.66	5.15	8.53	10.2	8.27	10.2	11.4	18.7	10.8	9.29	71.7	
Fe	664	61.4	3074	1925	709	569	2373	1231	2548	1322	846	1393	2881	
Pb	3.88	0.67	5.12	1.23	10.2	0.46	0.72	4.90	0.71	8.15	3.46	3.59	1.24	
Cu	10.9	3.5	29.1	17.6	12.4	2.44	53.0	33.1	2.30	14.5	8.63	17.0	53.5	
Zn	8.57	3.24	3.81	2.82	25.5	1.73	3.13	12.1	1.65	20.2	9.60	8.39	4.35	
Co	2.20	0.54	9.94	5.69	0.90	1.52	59.5	4.96	7.43	2.76	2.19	8.88	1.62	
Ni	81.8	34.2	311	281	9.59	33.3	1381	336	61.9	25.4	45.7	236	78.7	
K	86.8	7.35	350	81.8	33.0	84.8	72.6	30.1	133	76.3	79.0	94.0	22.4	
Cs	0.01	0.001	0.02	0.01	0.004	0.02	0.01	0.003	0.02	0.01	0.01	0.01	0.05	
Rb	0.45	0.03	1.08	0.47	0.10	0.47	0.55	0.11	0.94	0.27	0.37	0.44	0.10	
Ba	40.8	2.10	46.3	39.7	10.5	52.2	59.3	8.83	101	27.4	36.1	38.5	2.61	
La	1.37	0.05	2.90	1.63	0.31	1.12	2.27	0.42	2.34	0.84	1.08	1.30	4.25	
Ce	1.98	0.08	3.44	2.27	0.54	1.72	2.93	0.63	3.42	1.59	1.86	1.86	5.59	
Pr	0.18	0.01	0.32	0.23	0.06	0.19	0.27	0.11	0.37	0.15	0.16	0.19	0.60	
Nd	0.66	0.02	1.13	0.80	0.28	0.62	0.80	0.28	1.14	0.64	0.60	0.63	2.37	
Sr	4.34	0.17	20.8	6.35	0.87	13.8	5.20	2.62	12.8	4.43	6.01	7.03	15.4	
Sm	0.03	0.01	0.14	0.08	0.06	0.03	0.07	0.03	0.08	0.04	0.03	0.05	0.23	
Eu	0.003	0.001	0.05	0.02	0.001	0.003	0.02	0.001	0.02	0.003	0.004	0.01	0.06	
Gd	0.005	0.003	0.13	0.05	0.01	0.01	0.04	0.01	0.04	0.02	0.01	0.03	0.16	
Dy	0.003	0.0004	0.12	0.03	0.01	0.004	0.02	0.002	0.01	0.004	0.01	0.02	0.07	
Ho	0.0006	0.0003	0.02	0.003	0.004	0.0003	0.004	0.0005	0.003	0.001	0.002	0.004	0.01	
Y	6.72	0.06	3.55	3.84	7.83	0.16	0.10	15.2	0.14	14.6	4.10	5.12	0.30	
Er	0.003	0.0003	0.07	0.01	0.01	0.002	0.01	0.02	0.01	0.02	0.01	0.01	0.02	
Yb	0.17	0.001	0.15	0.06	0.18	0.002	0.01	0.23	0.01	0.36	0.09	0.11	0.02	
Lu	0.001	0.0001	0.01	0.001	0.002	0.0002	0.003	0.002	0.001	0.002	0.001	0.002	0.01	
V	1.48	0.07	2.74	2.19	0.37	7.10	9.19	1.65	9.90	2.51	2.62	3.62	4.23	
Ga	1.49	0.09	1.86	1.48	0.43	1.91	2.87	0.37	3.71	1.10	1.32	1.51	0.55	
Ti	6.26	4.66	12.9	5.94	4.26	5.92	18.1	4.24	23.3	11.3	4.98	9.26	615	
Zr	0.21	0.05	1.97	0.27	0.18	0.36	0.69	0.13	0.62	0.50	0.41	0.49	5.07	
Hf	0.004	0.002	0.04	0.004	0.004	0.01	0.01	0.01	0.02	0.02	0.01	0.01	0.15	
Nb	0.13	0.01	0.16	0.29	0.05	0.19	1.04	0.05	0.67	0.14	0.16	0.26	31.2	
Ta	0.01	0.0004	0.01	0.01	0.59	0.01	0.06	0.004	0.03	0.01	0.01	0.067	4.11	
Th	0.12	0.01	2.14	0.38	0.04	0.30	0.42	0.05	0.43	0.12	0.13	0.38	1.14	
U	0.005	0.001	0.02	0.01	0.01	0.01	0.07	0.003	0.02	0.01	0.01	0.01	0.44	

The walls of the open cavities are covered by euhedral diamond crystals; these are commonly simple octahedra, but octahedra with terraced faces are also present. The silicates are mostly interstitial or occupy space in cavities, and they often contain inclusions of euhedral diamonds, providing evidence for the cogenetic origin of diamond and silicates. The most common silicate is pyrope-almandine garnet, which occurs with a range of colours and chemical compositions (Kurat and Dobosi, 2000; Dobosi and Kurat 2002), i.e., orange and purple garnets similar to those found in the upper mantle eclogites and garnet peridotites, respectively (e.g., Nixon, 1987). Diopside is less common; olivine and orthopyroxene are notable by their absence (Kurat and Dobosi, 2000; Dobosi and Kurat 2002). As the main difference between the “peridotitic” and “eclogitic” garnets is in Cr content, the “peridotitic” to “eclogitic” range in the compositions of the silicate inclusions in the diamondites is consistent with precipitation from fractionating fluids/melts (Dobosi and Kurat, 2002).

Gurney and Boyd (1982) identified garnet, chromite, clinopyroxene and rutile intergrown with polycrystalline diamond. Ilmenite and dolomite have been identified in samples from Jwaneng (Kirkey et al., 1994). Jacob et al. (2004) report native Fe–Ni and FeS (troilite) and spherules of cohenite ( $\text{Fe}_3\text{C}$ ) in syngenetic garnet of eclogitic/pyroxenitic type in a polycrystalline diamond aggregate from the Venetia kimberlite.

The 11 diamondites analysed have been classified into peridotitic and eclogitic types based on the compositions of the intergrown garnet and clinopyroxene grains analysed by Dobosi and Kurat (2002)

and Kurat and Dobosi (2000); a more detailed description of the samples can be found in these papers.

### 3. Analytical techniques

Quantitative trace-element analyses of 38 elements in 11 diamondites have been carried out by LAM-ICPMS, using a multi-element-doped cellulose standard, as described by Rege et al. (2005); detection limits range to low-ppb levels for many elements.

Analysis of a synthetic (CVD) diamond has been used to identify and quantify molecular interferences, which have been treated as a “blank” and subtracted from the raw data (Rege et al., 2005). The analyses used a Brilliant 266 nm laser attached to an Agilent 7500 ICPMS; analytical conditions are detailed in Rege et al. (2005). Typical laser pits are 50–100  $\mu\text{m}$  in diameter and 25–35  $\mu\text{m}$  deep; analyses were done on roughly polished surfaces, and six to eight spots were analysed on each sample. Data were collected in time-resolved mode and reduced using the GLITTER software package (van Achterbergh et al., 2001), which allows selection of discrete intervals of the signal for integration and the calculation of concentrations.

As the diamond, silicates and other phases are intimately intergrown, it was difficult in many cases to obtain a clean analysis of the ‘diamond’ portion of the diamondites. A diamond with homogeneously distributed microinclusions will give a homogeneous time-resolved signal, representing the averaged composition of the

P-D054														
GP-2-Avg	GP-3-Avg	GP-4-Avg	GP-5-Avg	GP-6-Avg	GP-7-Avg	GP-8-Avg	P-D017-AVG	GP-1-Avg	GP-2-Avg	GP-3-Avg	GP-4-Avg	GP-5-Avg	GP-6-Avg	GP-7-Avg
2	3	4	5	2	3	3	24	9	8	8	8	7	4	4
39.7	80.8	31.1	15.5	15.8	138	36.3	49.2	35.1	30.7	20.9	11.1	18.0	782	546
2844	253	243	356	290	591	124	650	149	233	1964	25.0	117	1406	975
424	207	160	393	265	792	803	439	745	327	292	122	854	2526	2648
4141	1447	723	796	1126	1216	1375	2330	11086	1044	474	836	12317	11569	8828
42.7	4.10	3.93	7.73	3.55	11.7	5.77	18.9	61.1	10.7	3.16	5.56	72.6	29.1	59.5
3460	1681	1852	1601	2874	2275	367	2124	3429	1295	214	6935	3328	2749	2783
5.39	8.30	12.6	5.32	9.50	41.0	0.69	10.5	1.26	2.80	0.95	6.66	1.14	1.70	4.95
90.0	69.6	86.3	61.1	145	110	2.78	77.3	43.8	124	4.51	412	33.7	25.5	210
12.5	10.1	18.5	30.6	5.23	117	4.96	25.5	11.3	0.85	1.90	1.86	11.8	2.62	1.58
22.2	17.4	17.2	13.1	38.5	12.4	0.12	15.3	11.0	18.9	1.10	101	11.9	4.02	22.4
1323	909	1014	762	1857	731	4.34	835	695	941	21.4	5800	876	141	1079
670	82.0	69.5	110	207	124	11.8	162	67.3	52.8	105	228	31.6	164	185
0.16	0.06	0.02	0.02	0.07	0.02	0.03	0.05	0.07	0.01	0.01	0.03	0.05	0.18	0.20
3.70	0.44	0.27	0.49	1.13	0.39	0.04	0.82	0.70	0.19	0.34	0.72	0.22	1.11	1.02
72.0	27.3	42.4	30.7	70.9	32.8	2.44	35.1	35.2	7.93	10.4	27.5	18.6	35.2	68.0
7.07	3.46	2.03	1.89	5.15	1.30	4.85	3.75	1.82	1.01	1.24	2.83	1.58	3.61	8.73
8.97	4.34	2.70	2.49	6.29	1.80	6.38	4.82	2.62	1.58	1.79	4.09	2.32	6.09	13.0
0.75	0.40	0.24	0.23	0.58	0.19	0.74	0.47	0.29	0.19	0.19	0.42	0.29	0.64	1.39
2.32	1.20	0.67	0.64	1.52	0.95	2.81	1.56	1.05	0.64	0.58	1.57	1.21	2.65	4.98
42.1	157	71.9	33.4	98.4	14.5	24.7	57.2	14.1	6.64	4.34	9.54	11.5	35.3	37.1
0.16	0.07	0.05	0.05	0.11	0.08	0.37	0.14	0.17	0.12	0.05	0.12	0.22	0.39	0.51
0.03	0.01	0.003	0.004	0.01	0.01	0.09	0.03	0.05	0.02	0.01	0.02	0.06	0.10	0.10
0.08	0.02	0.01	0.01	0.02	0.02	0.25	0.07	0.16	0.04	0.03	0.05	0.20	0.25	0.28
0.05	0.01	0.003	0.003	0.01	0.01	0.11	0.03	0.17	0.03	0.01	0.03	0.20	0.20	0.14
0.01	0.0004	0.001	0.002	0.003	0.03	0.01	0.01	0.03	0.01	0.004	0.01	0.04	0.04	0.03
0.26	0.03	0.03	0.05	0.11	0.43	0.15	0.86	0.12	0.04	0.10	0.98	0.90	0.68	
0.03	0.005	0.002	0.001	0.002	0.01	0.05	0.01	0.12	0.01	0.002	0.02	0.13	0.11	0.07
0.04	0.002	0.002	0.002	0.003	0.01	0.04	0.01	0.17	0.01	0.004	0.01	0.18	0.08	0.06
0.01	0	0.0002	0.001	0.0003	0.002	0.02	0.004	0.04	0.002	0.002	0.003	0.03	0.01	0.01
9.19	0.66	0.72	1.65	1.22	1.27	0.37	2.41	2.34	0.56	1.50	1.88	2.62	5.53	4.17
4.29	1.53	2.38	1.78	4.17	1.93	0.20	2.10	1.66	0.32	0.83	0.90	1.00	1.66	2.39
60.4	5.73	8.07	8.10	11.0	14.4	6.37	91.2	36.4	9.20	74.5	6.27	27.8	95.2	190
1.36	0.49	0.19	0.27	0.42	0.35	0.21	1.04	0.74	0.29	0.37	0.38	0.78	1.86	1.64
0.03	0.01	0.004	0.01	0.01	0.01	0.02	0.03	0.01	0.03	0.01	0.01	0.01	0.07	0.05
1.02	0.19	0.17	0.19	0.63	0.13	0.34	4.24	4.17	0.18	0.36	0.31	3.68	1.02	3.34
0.06	0.01	0.02	0.02	0.04	0.03	0.15	0.55	0.11	0.04	0.03	0.02	0.14	0.16	0.36
0.91	0.59	0.26	0.41	0.59	0.27	0.69	0.61	0.68	0.71	0.30	0.52	0.54	1.62	1.57
0.06	0.03	0.03	0.03	0.04	0.04	0.05	0.09	1.44	0.03	0.06	0.10	1.50	0.10	0.15

(continued on next page)

microinclusions. Inclusions more than a few microns in diameter will appear as simultaneous "spikes" in several elements. Where such spikes were observed, we have selected and integrated these parts of

the time-resolved signal, differentiating these larger inclusions from the more homogeneous background. These analyses allow the semi-quantitative characterisation of individual inclusions. Several types of

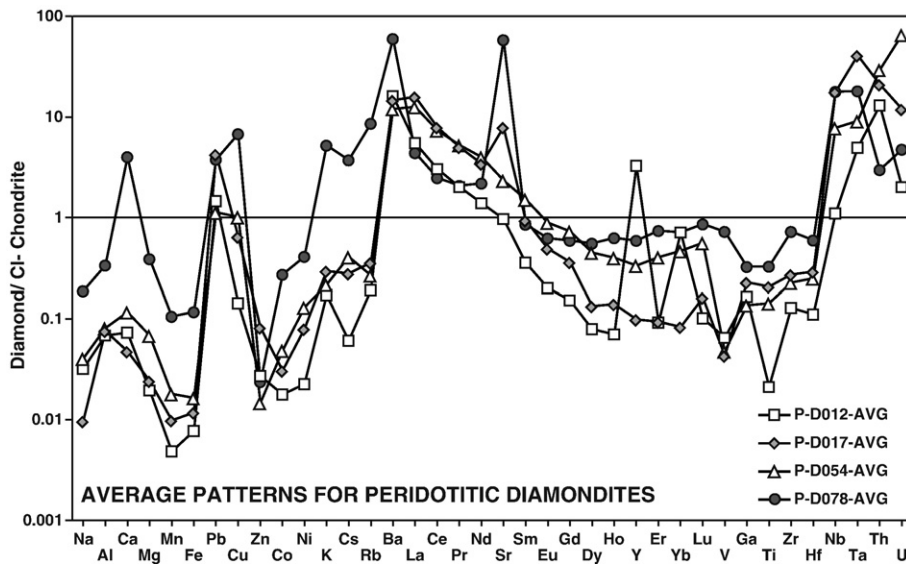


Fig. 1. Average chondrite-normalised trace-element patterns for peridotitic diamondites.

**Table 1** (continued)

Element	Peridotitic diamondites												Eclogitic diamondites	
	P-D054		P-D078										E-D001	
	P-D054-AVG	GP-1-Avg	GP-2-Avg	GP-3-Avg	GP-4-Avg	GP-5-Avg	GP-6-Avg	GP-7-Avg	GP-8-Avg	GP-9-Avg	GP-10-Avg	P-D078-AVG	GP-1-Avg	GP-2-Avg
No. of analyses	48	6	4	6	4	10	10	4	6	3	5	58	5	4
Na	206	259	508	44.5	371	1032	3001	403	3375	73.3	479	955	4154	39.8
Al	696	1274	2119	3710	878	2283	5248	2348	4174	4450	2431	2891	481793	2281
Ca	1073	2310	2481	1462	10058	19031	57249	26863	242599	2290	7048	37139	110380	799
Mg	6593	10363	22945	6761	19537	22797	73459	6084	40098	23398	150349	37579	718340	2715
Mn	34.5	51.7	106	77.2	72.5	226	425	82.0	339	99.1	544	202.3	10963	36.0
Fe	2962	2752	16150	4330	3687	101340	19028	4339	12682	18750	29139	21220	274252	2139
Pb	2.78	0.52	4.85	0.47	0.55	67.1	7.86	0.80	1.93	0.54	8.49	9.31	8.60	3.29
Cu	122	33.0	789.8	27.6	10.4	6040	234	176	612	78.5	124	812	2771	69.3
Zn	4.55	4.40	14.5	2.84	1.55	13.6	11.3	0.85	5.00	2.43	16.9	7.33	166	6.83
Co	24.3	4.80	61.8	6.05	5.80	1122	37.5	7.93	21.0	9.70	90.8	137	247	7.14
Ni	1365	104	2473	156	123	34533	1970	383	849	321	1986	4290	1408	347
K	119	289	2503	420	344	15424	3977	588	2095	1473	1492	2861	3104	107
Cs	0.08	0.05	0.39	0.05	0.05	5.07	0.53	0.09	0.30	0.11	0.44	0.71	0.44	0.005
Rb	0.61	2.11	16.5	3.26	3.08	99.4	31.5	4.40	13.7	11.4	11.7	19.7	31.6	0.51
Ba	29.0	16.4	46.5	28.9	31.9	66.8	213	57.9	815	105	52.4	143	79.2	11.2
La	2.97	0.05	0.12	0.04	0.19	1.28	4.63	0.32	2.81	0.30	0.70	1.04	7.21	0.34
Ce	4.50	0.08	0.14	0.05	0.24	2.29	7.80	0.36	2.98	0.39	0.87	1.52	14.7	0.48
Pr	0.49	0.01	0.02	0.02	0.03	0.30	1.00	0.05	0.36	0.04	0.09	0.19	2.09	0.07
Nd	1.81	0.06	0.27	0.27	0.15	1.45	4.16	0.39	2.51	0.22	0.51	1.00	10.0	0.33
Sr	16.9	4.96	14.2	5.97	91.5	52.6	133	355	3447	35.9	54.4	420	44.3	3.68
Sm	0.22	0.01	0.02	0.02	0.03	0.19	0.57	0.03	0.28	0.04	0.08	0.13	3.25	0.07
Eu	0.05	0.003	0.01	0.01	0.01	0.05	0.14	0.02	0.08	0.01	0.02	0.04	1.33	0.02
Gd	0.15	0.02	0.04	0.05	0.04	0.13	0.41	0.06	0.29	0.07	0.07	0.12	4.51	0.08
Dy	0.11	0.04	0.05	0.13	0.04	0.12	0.34	0.10	0.35	0.12	0.07	0.14	6.80	0.12
Ho	0.02	0.01	0.02	0.04	0.01	0.02	0.07	0.03	0.09	0.04	0.02	0.03	1.69	0.03
Y	0.53	0.24	0.44	0.86	0.24	0.56	1.73	0.79	3.00	0.97	0.48	0.93	38.9	0.70
Er	0.06	0.03	0.07	0.14	0.03	0.07	0.20	0.11	0.32	0.15	0.06	0.12	5.74	0.10
Yb	0.08	0.03	0.07	0.18	0.02	0.07	0.19	0.11	0.26	0.16	0.06	0.12	7.44	0.10
Lu	0.01	0.01	0.03	0.004	0.01	0.03	0.02	0.05	0.03	0.01	0.02	0.02	1.34	0.02
V	2.66	15.2	20.3	20.2	18.3	63.8	158	16.1	40.3	23.9	30.1	40.6	1582	20.9
Ga	1.25	0.56	1.30	0.90	0.85	1.96	5.72	1.35	13.5	2.46	1.41	3.00	36.8	0.72
Ti	62.7	47.9	103	82.2	43.2	146	366	64.5	224	235	129	144	21010	322
Zr	0.86	0.82	2.13	1.17	0.74	3.38	8.66	0.77	2.73	4.47	2.78	2.76	175	22.4
Hf	0.03	0.02	0.05	0.03	0.01	0.08	0.18	0.02	0.07	0.10	0.06	0.06	4.58	0.83
Nb	1.87	0.85	1.94	1.13	0.62	4.47	17.3	0.90	4.75	7.05	3.68	4.27	8.78	1.20
Ta	0.12	0.03	0.06	0.06	0.04	0.29	1.10	0.05	0.28	0.34	0.22	0.25	0.38	0.06
Th	0.85	0.01	0.01	0.004	0.01	0.10	0.53	0.01	0.06	0.03	0.10	0.09	0.65	0.02
U	0.48	0.01	0.02	0.003	0.003	0.04	0.17	0.01	0.03	0.02	0.05	0.04	1.41	0.03

trace-element pattern have been recognised, representing the different types of solid phases present in the diamondites (see Section 5.2). After the removal of these obvious inclusions, the

remaining more homogeneous portions of the signals have been taken as representing the diamond itself, with its submicroscopic fluid and solid inclusions.

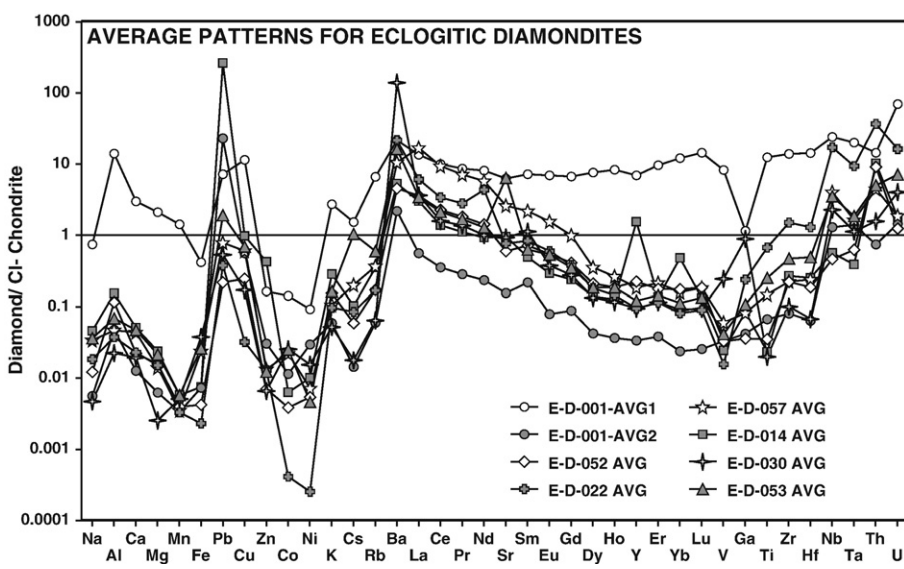


Fig. 2. Average chondrite-normalised trace-element patterns for eclogitic diamondites.

E-D014													
GP-5-Avg	GP-6-Avg	GP-7-Avg	GP-10-Avg	E-D-001-AVG1	GP-3-Avg	GP-4-Avg	GP-8-Avg	GP-9-Avg	E-D-001-AVG2	GP-1-Avg	GP-2-Avg	GP-3-Avg	GP-4-Avg
11	7	2	4	33	4	8	3	3	18	3	5	2	2
2163	431	2791	12304	3647	35.2	12.5	50.4	12.9	27.8	195	118	140	25.4
38657	4151	70592	97427	115817	555	302	268	456	395	2758	525	771	157
16619	1743	11564	19027	26689	207	59.9	93.2	94.1	113	819	342	320	61.7
215977	5257	105859	124968	195519	720	412	860	341	583	3697	1785	1292	261
2629.7	48.5	1156	898	2622	8.15	10.2	2.39	4.20	6.24	24.3	5.81	3.79	1.57
83265	5579	30843	40302	72730	2024	766	1396	922	1277	2578	854	678	506
9.15	12.12	8.60	60.4	17.0	14.1	200	1.83	3.45	54.7	2152	152	94.3	31.8
3557	246	606	677	1321	124	6.52	84.2	43.7	64.7	251	22.0	13.3	24.8
73.9	11.5	19.1	15.5	48.9	23.5	7.72	1.25	3.93	9.11	288	11.8	13.5	6.77
94.9	19.7	24.5	18.8	68.6	11.3	0.21	6.93	3.72	5.53	5.29	1.64	0.78	2.82
2370	1126	152	191	932	651	4.58	333	211	300	177	37.4	23.5	107
2491	116	694	2129	1440	64.5	11.7	25.8	22.9	31.2	223	179	62.0	18.5
0.37	0.01	0.14	0.70	0.28	0.01	0.001	0.002	0.002	0.003	0.03	0.01	0.005	0.002
21.4	114	6.37	26.7	14.6	0.30	0.04	0.10	0.09	0.13	0.94	0.78	0.24	0.09
108	11.4	12.6	75.8	49.8	15.6	1.41	1.82	1.52	5.08	21.2	20.6	3.14	1.03
6.69	0.56	0.77	2.98	3.09	0.15	0.03	0.22	0.11	0.13	1.32	0.95	0.20	0.08
11.8	1.01	1.44	5.91	5.89	0.28	0.05	0.33	0.19	0.21	1.49	1.02	0.29	0.11
1.54	0.15	0.19	0.61	0.77	0.03	0.01	0.04	0.02	0.03	0.19	0.13	0.03	0.01
6.56	0.71	0.89	2.78	3.55	0.16	0.03	0.16	0.07	0.10	0.72	0.52	0.14	0.05
49.3	11.9	20.1	134	43.8	1.88	0.29	1.28	0.91	1.09	11.0	8.16	3.57	0.52
1.41	0.13	0.33	0.96	1.02	0.06	0.01	0.03	0.02	0.03	0.13	0.09	0.03	0.01
0.49	0.03	0.13	0.25	0.38	0.01	0.001	0.01	0.003	0.004	0.03	0.02	0.01	0.001
1.47	0.11	0.54	0.99	1.28	0.03	0.003	0.01	0.02	0.02	0.09	0.07	0.02	0.01
1.73	0.14	0.79	1.21	1.80	0.02	0.004	0.01	0.003	0.01	0.06	0.04	0.01	0.002
0.39	0.03	0.20	0.28	0.44	0.004	0.001	0.002	0.001	0.002	0.01	0.01	0.003	0.0002
9.12	0.93	4.71	8.52	10.5	0.09	0.03	0.06	0.03	0.05	8.53	0.80	0.53	0.22
1.27	0.13	0.70	0.93	1.48	0.01	0.002	0.01	0.004	0.01	0.04	0.02	0.01	0.002
1.51	0.12	0.93	1.11	1.87	0.01	0.001	0.004	0.002	0.004	0.24	0.03	0.02	0.01
0.27	0.02	0.16	0.22	0.34	0.001	0.001	0.0004	0.0005	0.001	0.01	0.003	0.001	0.0001
712	8.21	163	184	445	2.36	1.11	2.88	0.80	1.79	1.65	2.78	1.20	0.14
10.6	0.82	5.19	7.15	10.2	0.99	0.16	0.17	0.17	0.37	1.31	1.21	0.22	0.07
6127	108	1953	2020	5257	77.0	13.5	12.1	11.0	28.4	15.8	10.6	5.63	1.69
59.3	3.27	21.0	26.8	51.3	0.80	0.09	0.21	0.09	0.30	1.40	0.73	0.35	0.20
1.65	0.08	0.61	0.72	1.41	0.02	0.001	0.003	0.001	0.01	0.03	0.02	0.01	0.003
18.0	0.57	1.24	3.49	5.55	0.79	0.05	0.27	0.09	0.30	0.17	0.24	0.03	0.01
0.88	0.04	0.06	0.15	0.26	0.06	0.003	0.01	0.003	0.02	0.01	0.01	0.003	0.001
0.93	0.09	0.12	0.60	0.40	0.03	0.01	0.04	0.01	0.02	0.46	0.25	0.08	0.05
1.24	0.02	0.10	0.16	0.49	0.02	0.01	0.04	0.01	0.03	0.01	0.01	0.002	

(continued on next page)

The diamond analyses for each sample were divided into groups based on the visual similarity of their trace-element patterns. The averages of each group are given in Table 1; as well as the average for each diamondite, the complete data set is presented in the Data Repository. Average values (see Data Repository) are presented in the form of chondrite-normalised trace-element abundance patterns ("spidergrams"; normalising values from McDonough and Sun, 1995). The order in which the elements are presented is based on their ionic radii, valence and chemical affinity.

## 4. Results

### 4.1. "Peridotitic" diamondites

The trace-element patterns of the "peridotitic" diamondites (Fig. 1) show enrichment of the LREE compared to the MREE with abundances continuously decreasing from Ba to Ho. Pb and Cu are enriched relative to Fe. Ti, Zr and Hf are depleted, and Nb, Ta, Th and U are enriched, relative to chondrites. Ca/Mg and Mg/Fe are higher than chondritic values; K, Rb and Cs are low relative to Ba. Apart from these common features, some of the samples show individual characteristics. Dia-012 shows very strong positive anomalies in Y and Yb, and a negative anomaly in Ti. Dia-017 shows a positive anomaly in Sr. Dia-078 has notably higher levels of the "major" elements (Na–Fe), high K, Cs, Rb and Ba, and a strong positive anomaly in Sr.

### 4.2. "Eclogitic" diamondites

Most of the averaged patterns for the "eclogitic" diamondites are similar to those of the "peridotitic" diamondites, showing enrichment of the LREE compared to the MREE with abundances continuously decreasing from Ba to Ho (Fig. 2). The striking exception is E-D-001, in which different areas display one of two very different patterns. The first set (Avg-1; 33 analyses) has an almost flat REE pattern with higher HREE and MREE than the other samples, but similar levels of Ba, La and Ce. This set also has higher contents of the "major" elements (Na–Fe), K–Rb–Cs, and the HFSE, but shows a pronounced negative anomaly in Ga. The patterns for the second set (Avg-2; 18 analyses) are generally similar to those of the other samples.

On an individual basis, Dia-014 shows positive anomalies in Y, Yb and Pb and a negative Ti anomaly. Dia-030 has very high Ba, Sr and Ga abundances and a prominent negative Ti anomaly. Dia-053 shows high Cs relative to K and Rb and a positive Sr anomaly, whereas Dia-022 shows low Co and Ni abundances.

## 5. Discussion

### 5.1. Fluid composition

The diamondite analyses are inferred to represent a mixture of the trapped fluid/melt from which they have grown and submicroscopic

**Table 1** (continued)

Element	Eclogitic diamondites													
	E-D014			E-D022						E-D030				
	GP-5-Avg	GP-6-Avg	E-D014-AVG	GP-1-Avg	GP-2-Avg	GP-3-Avg	GP-4-Avg	GP-5-Avg	GP-6-Avg	GP-7-Avg	E-D-022 AVG	GP-1-Avg	GP-2-Avg	GP-3-Avg
No. of analyses	2	8	22	4	11	6	3	2	5	10	41	5	13	2
Na	235	651	228	33.8	168	38.2	243	99.5	27.7	27.2	91.1	13.6	65.0	19.3
Al	790	2695	1283	83.0	899	177	944	23.7	45.0	15.8	312	233	474	127
Ca	385	795	454	69.5	509	88.0	632	27.6	96.2	13.2	205	121	454	176
Mg	3087	3248	2228	469	4084	631	4483	25.1	144	35.6	1410	363	575	188
Mn	15.6	13.3	10.7	1.93	15.6	8.47	15.6	0.41	0.59	0.27	6.12	12.4	32.4	4.81
Fe	1320	1991	1321	166	1105	351	1101	34.1	64.3	21.7	406	4073	27079	1976
Pb	24.5	1285	623	0.47	0.27	2.06	1.67	0.95	0.45	0.43	0.90	0.27	3.03	1.35
Cu	31.5	337	113	1.41	6.72	1.08	10.4	2.82	2.19	1.45	3.73	6.50	68.3	5.07
Zn	9.27	434	127	3.11	2.91	3.10	9.41	4.40	2.47	1.72	3.88	1.51	3.50	1.70
Co	3.28	4.51	3.05	0.10	0.43	0.13	0.36	0.20	0.06	0.13	0.20	8.03	48.4	3.90
Ni	100	168	102	1.25	4.78	1.60	3.94	4.78	0.64	1.20	2.60	50.7	640	25.5
K	134	294	152	52.3	65.6	26.3	122	49.0	27.5	21.2	51.9	23.6	70.7	33.7
Cs	0.01	0.06	0.02	0.01	0.03	0.02	0.04	0.001	0.01	0.0002	0.02	0.004	0.01	0.005
Rb	0.66	1.97	0.78	0.25	0.58	0.30	1.24	0.06	0.16	0.03	0.37	0.10	0.42	0.14
Ba	9.45	18.3	12.3	37.1	43.4	181	78.4	1.40	8.13	1.38	50.1	4.14	263	3.92
La	0.89	0.67	0.69	0.25	1.14	5.50	2.09	0.02	0.72	0.02	1.39	0.61	2.98	0.47
Ce	1.26	0.74	0.82	0.28	1.46	8.64	2.40	0.04	1.21	0.04	2.01	0.81	3.23	0.47
Pr	0.14	0.09	0.10	0.03	0.18	1.02	0.33	0.04	0.15	0.004	0.25	0.11	0.40	0.08
Nd	0.63	0.39	0.41	0.14	0.68	3.59	7.96	0.47	0.51	0.03	1.91	0.43	1.47	0.23
Sr	3.27	13.8	6.72	1.72	9.78	6.27	15.2	0.19	3.86	0.23	5.33	2.14	12.3	2.13
Sm	0.09	0.07	0.07	0.02	0.12	0.43	0.20	0.01	0.07	0.002	0.12	0.06	0.23	0.55
Eu	0.02	0.01	0.02	0.01	0.03	0.12	0.04	0	0.03	0.0005	0.03	0.02	0.06	0.01
Gd	0.06	0.04	0.05	0.01	0.07	0.27	0.11	0.01	0.05	0.001	0.07	0.04	0.18	0.04
Dy	0.06	0.02	0.03	0.01	0.04	0.19	0.04	0.002	0.01	0.001	0.04	0.02	0.12	0.01
Ho	0.01	0.005	0.01	0.001	0.007	0.03	0.008	0	0.006	0.0003	0.008	0.004	0.02	0.002
Y	0.36	3.56	2.34	0.02	0.18	0.49	0.16	0.003	0.15	0.005	0.14	0.09	0.52	0.05
Er	0.03	0.02	0.02	0.002	0.015	0.08	0.01	0.0005	0.007	0.001	0.018	0.01	0.07	0.01
Yb	0.03	0.12	0.07	0.002	0.011	0.06	0.01	0	0.001	0.0002	0.013	0.01	0.06	0.01
Lu	0.004	0.003	0.003	0.0003	0.002	0.01	0.003	0.001	0.0004	0.0001	0.0021	0.001	0.01	0.001
V	0.85	1.33	1.32	0.32	1.93	1.17	2.11	0.18	0.17	0.06	0.85	4.47	59.2	2.91
Ga	0.58	1.13	0.75	1.37	1.62	5.72	3.16	0.05	2.87	0.07	2.12	0.20	7.33	0.19
Ti	12.5	13.7	10.0	20.9	13.3	1868	51.1	1.89	31.0	10.1	285	14.6	25.8	3.86
Zr	2.32	0.94	0.99	0.87	2.82	29.7	4.45	0.09	0.85	0.10	5.55	0.31	1.34	0.15
Hf	0.06	0.03	0.03	0.02	0.07	0.69	0.10	0.002	0.01	0.00	0.13	0.01	0.02	0.003
Nb	0.19	0.15	0.13	0.22	0.02	20.6	4.01	0.01	2.81	0.04	3.97	0.72	1.62	0.26
Ta	0.001	0.01	0.01	0.01	0.00	0.79	0.03	0.01	0.01	0.01	0.12	0.04	0.03	0.01
Th	0.68	0.20	0.29	0.07	0.35	6.07	0.51	0.01	0.14	0.01	1.02	0.07	0.10	0.03
U	0.01	0.01	0.01	0.01	0.01	0.71	0.05	0.002	0.02	0.005	0.12	0.02	0.11	0.01

solid phases (including diamond and intergrown silicates±other solid phases) that crystallised out of the fluid, either as daughter phases in fluid/melt inclusions or as discrete microphases. To test whether the fluid compositions represented by the diamondite analyses (after excluding obvious macro-inclusions) are realistic, the trace-element compositions of fluids in equilibrium with the garnet and clinopyroxene analysed by Dobosi and Kurat (2002) were calculated for an extended range of elements. The partition coefficients between garnet, clinopyroxene and kimberlite melt of Fujimaki et al. (1984) were used for La, Ce, Nd, Sm, Eu, Gd, Dy, Er, Yb, Lu, Zr, Hf and Pb. Coefficients between garnet, clinopyroxene and basaltic melts for the remaining elements were taken from Jenner et al. (1993) and Hauri et al. (1994); see Table 2. Preference was given to partition coefficients for kimberlitic melts wherever possible, as they represent an environment that is similar in pressure and temperature conditions to that inferred for the formation of diamondites. Fluid compositions were calculated for 5 diamondite samples; two “peridotitic” and three “eclogitic”; trace-element compositions of garnet and/or clinopyroxene in these samples are given by Kurat and Dobosi (2000) and Dobosi and Kurat (2002).

### 5.1.1. Fluid compositions for “peridotitic” diamondites

Fig. 3 shows the average analyses for peridotitic diamondite samples Dia-012 and Dia-017, compared with the hypothetical fluids calculated from garnet (and clinopyroxene in the case of sample Dia-012). As described by Kurat and Dobosi (2000) the garnet and clinopyroxene are intimately intergrown with each other and with

diamond, indicating syngenetic crystallisation. Therefore the fluid composition calculated from the coexisting garnet and clinopyroxene should be the same; differences between the calculated fluids can be attributed to inappropriate partition coefficients for some elements. These calculated values were averaged and divided by 100 for comparison with the diamondite data. The absolute concentrations of the elements in the diamondite-forming fluid cannot be determined unequivocally, because the relative abundance of inclusions is unknown. However, comparison between calculated and analysed values indicates that the fluid (±solid) inclusions make up roughly 1% by weight of the polycrystalline diamond aggregate.

For sample Dia-012, the shape of the pattern of the calculated fluid matches the diamondite analyses quite closely, but the analyses have positive Y and Yb anomalies that are not seen in the calculated fluid. Other notable differences between the calculated fluid and the diamondite analysis include high Ti and Nb, and low Ta and Th. The diamondite pattern shows higher Al–Ca–Mg–Mn–Fe than the calculated fluid, compared to elements such as the REE. This may be due to the choice of basalt-derived distribution coefficients for these elements, or to the presence of submicroscopic garnet and clinopyroxene, which were ablated with the diamond. This would lead to a slightly enriched pattern compared to the hypothetical fluid; for example, garnet would enrich HREE, clinopyroxene the LREE.

The hypothetical fluid calculated for Dia-017 (using only garnet, as no clinopyroxene was found in this sample) is a reasonable match for the analysed diamondite except for the LREE, which are slightly lower,

E-D052												E-D053		
GP-4-Avg	GP-5-Avg	GP-6-Avg	E-D-030 AVG	GP-1-Avg	GP-2-Avg	GP-3-Avg	GP-4-Avg	GP-5-Avg	GP-6-Avg	E-D-052 AVG	GP-1-Avg	GP-2-Avg	GP-3-Avg	
3	4	7	34	18	3	6	4	7	4	42	5	3	7	
10.4	3.07	27.9	23.2	103	106	4.79	28.5	103	16.2	60.4	96.0	340	187	
83.8	29.0	176.0	187	1987	1003	40.3	245	2333	160	961	424	972	754	
43.1	30.6	218.1	174	399	247	26.2	103	374	53.2	200	476	712	367	
91.5	29.4	191	240	3207	1463	111	416	3148	469	1469	1735	4229	2044	
1.95	0.94	4.62	9.52	8.67	11.08	0.80	4.87	15.6	3.11	7.36	11.5	13.2	17.0	
2341	423	3929	6637	1213	454	51.1	820	1312	577	738	7853	5943	5302	
0.13	0.31	2.51	1.27	0.49	0.96	0.38	0.64	0.51	0.14	0.52	3.00	5.44	3.58	
18.8	1.00	20.0	19.9	59.6	18.8	6.17	40.6	12.8	32.6	28.4	151	154	34.1	
0.41	0.45	4.30	1.98	2.60	5.07	0.75	1.12	2.27	0.85	2.11	3.10	5.48	4.07	
5.82	0.77	7.33	12.4	2.06	0.43	0.04	4.97	0.92	2.75	1.86	23.8	16.8	10.7	
101	7.14	123	158	47.3	4.78	0.95	166	18.1	94.0	55.1	103	72.2	24.6	
15.4	4.99	19.1	27.9	88.1	86.1	25.5	46.9	229	14.7	81.7	97.2	157	45.9	
0	0	0.002	0.003	0.02	0.01	0.002	0.005	0.03	0.001	0.01	0.23	0.22	0.10	
0.08	0.03	0.09	0.14	0.40	0.40	0.10	0.22	1.09	0.09	0.38	1.35	2.26	1.03	
20.6	18.3	1632	324	17.8	10.1	1.74	4.45	27.2	1.80	10.5	29.3	33.9	75.8	
0.16	0.10	0.69	0.84	2.23	0.74	0.12	0.37	1.20	0.25	0.82	1.09	1.56	0.47	
0.23	0.12	0.75	0.94	3.58	1.23	0.13	0.52	1.87	0.68	1.34	1.61	2.75	0.72	
0.02	0.02	0.11	0.12	0.42	0.15	0.02	0.05	0.24	0.09	0.16	0.21	0.31	0.09	
0.08	0.06	0.38	0.44	1.67	0.59	0.05	0.23	1.02	0.20	0.63	0.86	1.07	0.34	
1.27	0.93	20.6	6.55	8.92	4.46	0.67	2.27	7.75	0.91	4.16	8.08	43.4	89.0	
0.01	0.01	0.10	0.16	0.26	0.07	0.01	0.04	0.18	0.05	0.10	0.14	0.17	0.04	
0.004	0.002	0.03	0.02	0.08	0.02	0.002	0.01	0.05	0.01	0.03	0.04	0.05	0.02	
0.01	0.01	0.04	0.05	0.20	0.06	0.01	0.02	0.15	0.02	0.08	0.11	0.12	0.04	
0.005	0.003	0.03	0.03	0.12	0.03	0.003	0.02	0.10	0.02	0.05	0.06	0.07	0.04	
0.001	0.001	0.005	0.01	0.02	0.006	0.0003	0.005	0.02	0.01	0.01	0.01	0.02	0.01	
0.03	0.03	0.14	0.14	0.98	0.21	0.01	0.12	0.59	0.13	0.34	0.25	0.25	0.15	
0.005	0.002	0.01	0.02	0.07	0.02	0.003	0.01	0.05	0.01	0.03	0.03	0.03	0.02	
0.001	0.002	0.01	0.01	0.06	0.03	0.002	0.02	0.05	0.01	0.03	0.01	0.02	0.02	
0.0002	0.0001	0.002	0.002	0.01	0.003	0.0002	0.002	0.01	0.001	0.004	0.003	0.004	0.004	
2.30	0.97	9.56	13.2	1.94	1.51	0.34	1.13	5.16	0.60	1.78	3.59	4.14	1.97	
0.71	0.62	38.3	7.89	0.56	0.30	0.06	0.17	0.77	0.07	0.32	0.87	0.97	1.74	
1.04	1.19	4.91	8.56	15.3	10.5	1.45	5.82	53.4	3.44	15.0	83.5	60.3	214	
0.17	0.05	0.23	0.37	1.84	0.84	0.06	0.25	1.78	0.16	0.82	2.29	2.98	1.61	
0.002	0.0003	0.005	0.01	0.04	0.02	0.001	0.01	0.04	0.003	0.02	0.06	0.10	0.04	
0.09	0.10	0.38	0.53	0.13	0.06	0.01	0.04	0.37	0.02	0.11	1.28	0.74	1.67	
0.001	0.004	0.01	0.01	0.01	0.02	0.003	0.002	0.02	0.001	0.01	0.03	0.04	0.02	
0.01	0.01	0.03	0.04	1.06	0.13	0.02	0.07	0.19	0.05	0.25	0.24	0.27	0.08	
0.01	0.002	0.02	0.03	0.02	0.01	0.002	0.005	0.01	0.004	0.01	0.06	0.09	0.07	

(continued on next page)

and the HREE, where the abundances are low compared to the diamondite analyses (Fig. 3). The diamondite analyses also show a positive Sr anomaly whereas the calculated fluid has a negative anomaly; this may reflect a problem with the choice of a garnet/melt partition coefficient for Sr, as well as the presence of a Sr-rich phase in the diamond analysis.

### 5.1.2. Fluid compositions for “eclogitic” diamondites

For sample Dia-001, the diamondite patterns define two groups and an average for each group was considered (Avg-1 and Avg-2; Fig. 4); melt was calculated for each group (data in Table 3) using garnet/melt distribution coefficients. The analyses represented by Avg-2 match the calculated fluid quite well. The analyses represented by Avg-1 show high MREE and HREE, and are similar to the trace-element pattern of garnet (Dobosi and Kurat, 2002). The addition of 80% garnet to the hypothetical fluid produces a pattern that matches the HREE and the HFSE levels of the diamondite analyses more closely (Fig. 4). These garnet-dominated patterns suggest that some analyses represent the portions of the diamondite where diamond + fluid were analysed, and the others represent volumes in which submicroscopic garnet was too finely dispersed to avoid during analysis, or to eliminate during data processing.

For sample Dia-014, the hypothetical fluid calculated from the garnet is generally similar to the average diamondite analysis, but the diamondite analyses show higher LREE than the calculated fluid, and positive anomalies in Y and Yb. The negative Sr anomaly in the

calculated fluid pattern is not observed in the sample; as noted above, the garnet/melt coefficient for Sr may not be appropriate. The observed Th abundance is also higher than that of the hypothetical fluid.

For sample Dia-030, the calculated fluid shows a generally good match with the observed REE patterns.

### 5.2. Other (inferred) phases

Although there is generally a good match between the calculated and observed ‘fluid/melt’ patterns for many elements, there are several notable anomalies. The most obvious are the large positive anomalies in Y and Yb in some diamondite analyses. Individual analyses also show negative Ti anomalies, positive Sr and Ga anomalies and unusually high abundances of Ba, Th, U and Pb. In the present work, a detailed study of the time-resolved plots of the diamondite analyses reveals numerous correlations between the enrichments of different elements. The presence of such element associations, and the differences between the calculated and observed fluids, suggest the presence of additional mineral phases in the diamondite, which contribute to the observed trace-element characteristics of the analyses.

The high Cu–Pb–Zn and Co–Ni abundances in some of the diamondite analyses (Fig. 5) suggest the presence of a sulfide phase. Although sulfides have not been identified in diamondites, except for FeS (troilite) in framesites from Venetia (Jacob et al., 2004), they are

**Table 1** (continued)

Element	Eclogitic diamondites											
	E-D053			E-D057								
	GP-5-Avg	GP-6-Avg	E-D-053 AVG	GP-1-Avg	GP-2-Avg	GP-3-Avg	GP-4-Avg	GP-5-Avg	GP-6-Avg	GP-7-Avg	GP-8-Avg	E-D-057 AVG
No. of analyses	15	11	41	4	8	7	11	5	5	4	2	46
Na	179	92.8	179	105	57.8	200	246	130	163	231	212	168
Al	263	448	572	112	151	193	611	281	203	1235	344	391
Ca	146	418	424	326	136	398	550	432	480	545	265	392
Mg	645	1419	2014	283	589	553	1849	970	465	4748	967	1303
Mn	3.39	8.57	10.7	3.29	4.56	4.80	11.3	5.78	4.72	13.6	4.26	6.53
Fe	1422	2337	4572	2168	3916	3036	6400	4090	2438	7466	3731	4155
Pb	2.31	8.28	4.52	1.13	1.44	0.97	0.53	1.30	3.01	1.81	4.78	1.87
Cu	32.4	26.7	79.7	52.0	79.5	64.6	82.3	71.1	58.6	74.8	76.1	69.9
Zn	4.29	1.52	3.69	2.67	2.46	3.12	2.98	1.88	7.67	2.56	8.41	3.97
Co	4.29	5.59	12.2	7.54	11.7	10.2	17.4	10.7	8.25	10.0	9.64	10.7
Ni	25.2	10.7	47.2	55.0	83.8	72.5	103	71.9	60.1	63.8	73.3	73.0
K	91.0	46.5	87.6	29.4	28.6	26.2	62.1	33.0	65.6	80.5	125	56.3
Cs	0.19	0.22	0.19	0.17	0.01	0.01	0.02	0.01	0.02	0.02	0.02	0.04
Rb	0.86	1.12	1.32	2.29	0.30	0.24	0.73	0.41	0.37	1.62	0.56	0.81
Ba	27.7	21.6	37.7	23.2	16.2	13.8	19.1	24.1	10.6	73.2	16.3	24.6
La	0.34	0.46	0.78	0.37	1.03	3.12	6.34	2.93	0.47	13.6	2.76	3.82
Ce	0.48	0.70	1.25	0.53	1.43	4.50	9.82	4.07	0.75	19.3	3.80	5.53
Pr	0.06	0.09	0.15	0.06	0.18	0.52	1.14	0.47	0.09	2.16	0.46	0.63
Nd	0.24	0.34	0.57	0.25	1.09	2.05	4.56	1.82	0.38	8.30	1.93	2.55
Sr	24.2	58.5	44.6	8.37	5.22	15.0	4.89	24.8	17.2	15.5	54.2	18.1
Sm	0.04	0.06	0.09	0.04	0.11	0.27	0.56	0.25	0.06	0.99	0.23	0.31
Eu	0.01	0.02	0.03	0.01	0.03	0.07	0.15	0.06	0.01	0.28	0.07	0.08
Gd	0.03	0.04	0.07	0.02	0.06	0.17	0.32	0.16	0.04	0.63	0.13	0.19
Dy	0.01	0.04	0.04	0.01	0.04	0.05	0.11	0.07	0.01	0.29	0.08	0.08
Ho	0.003	0.01	0.01	0.003	0.01	0.01	0.02	0.01	0.01	0.04	0.01	0.01
Y	0.06	0.21	0.18	0.03	0.16	0.16	0.36	0.25	0.05	0.96	0.26	0.28
Er	0.01	0.03	0.02	0.002	0.02	0.02	0.04	0.03	0.01	0.12	0.03	0.03
Yb	0.005	0.03	0.02	0.002	0.02	0.01	0.02	0.02	0.004	0.08	0.04	0.02
Lu	0.001	0.004	0.003	0.0004	0.004	0.002	0.003	0.004	0.003	0.01	0.01	0.004
V	0.75	0.86	2.26	1.63	1.02	2.49	7.90	3.14	2.18	6.45	1.16	3.24
Ga	0.67	0.53	0.96	0.62	0.44	0.44	0.76	0.61	0.31	2.23	0.45	0.73
Ti	167	12.9	108	12.9	35.7	27.9	94.5	83.0	26.9	168	53.6	62.8
Zr	0.88	0.90	1.73	0.47	0.40	0.51	0.97	0.98	0.46	2.29	0.56	0.83
Hf	0.02	0.02	0.05	0.02	0.01	0.02	0.03	0.02	0.02	0.06	0.01	0.02
Nb	0.28	0.12	0.82	0.03	0.32	0.22	1.06	1.27	0.19	3.83	0.57	0.94
Ta	0.03	0.005	0.02	0.002	0.01	0.01	0.03	0.02	0.01	0.06	0.03	0.02
Th	0.05	0.07	0.14	0.02	0.08	0.08	0.12	0.12	0.03	0.41	0.12	0.12
U	0.01	0.02	0.05	0.002	0.01	0.004	0.02	0.01	0.01	0.04	0.01	0.01

very commonly found as inclusions in diamonds (e.g. Meyer, 1987; Harris, 1992).

One of the most likely additional phases is a carbonate enriched in Ca–Mg–Ba–Sr, the presence of which could account for the high Ba and Sr contents seen in some analyses. Such carbonates have been reported in a cloudy diamond from Udachnaya (Schrauder and Navon, 1993), in diamonds from Koffiefontein, RSA (Izraeli et al., 2004) and from Siberia, South Africa, China and Canada (Leung, 1984, 1990; Bulanova and Pavlova, 1987; Wang et al., 1996; Davies et al., 1999; McDade and Harris, 1999). Ca–Mg–Fe carbonates have also been found as secondary phases in fluid inclusions in fibrous diamonds (Guthrie et al., 1991; Walmsley and Lang, 1992).

Kirkley et al. (1994) identified dolomite inclusions in framesites from Jwaneng. They also describe secondary white carbonates forming a coat, and occurring in cracks, vugs and interstices of more porous samples. However, such secondary carbonates are unlikely to be enriched in Sr, Ba or REE. Although no trace-element analyses of carbonate found as inclusions in diamondites or diamondites are available, Bühn and Rankin (1999) identified carbonates rich in REE, Sr, Ba and Y, which occur as solid phases in carbonatite-derived fluid inclusions in the country rocks of the Kalkfeld carbonatite complex, Namibia. van Achterbergh et al. (2002, 2004) describe quenched carbonate–silicate melt inclusions in herzolitic clinopyroxene macro-crysts derived from 180 to 200 km beneath the Slave craton in northern Canada. These inclusions are interpreted as natural samples of mantle carbonatites, and the carbonates are rich in LREE, Ba and Sr.

Many of the diamondite analyses show a strong positive anomaly in Y (relative to the heavy REE); a smaller, but correlated, positive Yb anomaly is also seen in many of these analyses (Fig. 6). The positive Y anomaly may be explained by the presence of a fluoride phase; analyses of fluorite show the presence of a very strong positive Y anomaly and some also show a positive Sr anomaly (e.g. S. Jackson, pers. comm. — positive Y; Bühn et al., 2002 — fluorite from carbonatite, showing positive Sr). Some of these inclusions also show LREE enrichment similar to that of fluorapatite, another F-bearing phase. Klemme (2004) reports the presence of fluoride phases in metasomatised mantle xenoliths, which were detected only after they had been preserved by careful polishing of the samples with a nonhydrous polishing liquid. Such fluorides may have not been previously detected as they have been lost during sample preparation. Unfortunately, F could not be determined by our analytical method.

Correlated anomalous enrichments in Al, K, Ba, Nb, Ta and Cs suggest that a mica phase may also be present. Izraeli et al. (2004) have identified phlogopite and high-silica mica in cloudy diamonds from Koffiefontein. van Achterbergh et al. (2004) also report phlogopite rich in Ba, Sr, Nb and Ta in the carbonatite blebs from the lower lithosphere of the Slave Craton, as discussed above.

LIMA minerals (Lindsleyite–Mathiasite; K–Ba–Zr–Cr titanates) have been reported in mantle xenoliths and heavy mineral concentrates from a number of kimberlites in Southern Africa and China (Haggerty, 1983; Haggerty, 1987; Zhou et al., 1984). These phases show strong enrichment in the LREE and the HFSE (with high Ti) and

**Table 2**

Partition coefficients for garnet and clinopyroxene used for fluid calculation (bold text)

Dgnt/liq	Dcpx/liq					
Element	Fujimaki et al. (1984) <sup>a</sup>	Jenner et al. (1993) <sup>b</sup>	Hauri et al. (1994) <sup>c</sup>	Fujimaki et al. (1984) <sup>a</sup>	Jenner et al. (1993) <sup>b</sup>	Hauri et al. (1994) <sup>c</sup>
Na	<b>0.04</b>					
Al	<b>1.54</b>					
Ca	<b>1.14</b>					
Mg	<b>2.58</b>					
Mn						
Fe	<b>1.65</b>					
Pb		<b>0.00012</b>	0.014		0.0102	
Ba		<b>0.0007</b>			0.0058	
La	<b>0.0001</b>		0.0164	<b>0.023</b>		0.052
Ce	<b>0.0051</b>		0.065	<b>0.033</b>		0.108
Pr	<b>0.011<sup>d</sup></b>					
Nd	<b>0.025</b>		0.363	<b>0.063</b>		0.277
Sr		<b>0.01</b>	0.0099		<b>0.06</b>	0.157
Sm	<b>0.088</b>		1.1	<b>0.123</b>		0.462
Eu	<b>0.131</b>		2.02	<b>0.135</b>		0.458
Gd	<b>0.260</b>			<b>0.165</b>		
Dy	<b>1.11</b>		4.13	<b>0.305</b>		0.711
Ho						0.660
Y		<b>4.20</b>			<b>0.900</b>	
Er	<b>2.99</b>		3.95	<b>0.460</b>		0.660
Yb	<b>5.24</b>		3.88	<b>0.427</b>		0.633
Lu	<b>5.98</b>		3.79	<b>0.435</b>		0.623
V		<b>3.45</b>	1.48			1.81
Ga						
Ti		0.65	0.688		<b>0.430</b>	0.451
Zr	<b>0.240</b>		2.12	<b>0.306</b>		
Hf	<b>0.207</b>			<b>0.262</b>		
Nb		<b>0.015</b>	0.0538			0.0081
Ta		<b>0.051</b>			<b>0.005</b>	
Th			<b>0.00137</b>			0.0130
U			<b>0.00588</b>			0.0127

<sup>a</sup> Fujimaki et al. (1984), kimberlite, high P run product, 1150 °C, 2 GPa.

<sup>b</sup> Jenner et al. (1993), basalt, 1100 °C, 25 kbar.

<sup>c</sup> Hauri et al. (1994), basalt, 14,300 °C, 2.5 GPa.

<sup>d</sup> Klemme et al. (2002), Fe-free "basalt", 1200 °C, 3 GPa.

have positive anomalies in Yb and Sr (authors' unpublished data). The presence of such a phase in the diamondites could account for some of the observed anomalies, especially in Yb.

The presence of chromite (previously reported in diamondites by Gurney and Boyd, 1982 and Kirkley et al., 1994) in these samples

would only affect the abundance of chromium, as this mineral does not host significant amounts of REE or HFSE. This could not be verified as Cr was not analysed due to molecular interferences. The presence of a phase such as ilmenite may explain anomalies in the Ti, Nb and Ta abundances of some diamondite analyses.

### 5.3. Crystal fractionation and fluid evolution

Modelling of geochemical processes and the evolution of magmatic rocks is usually carried out using trace-element abundances. In the case of the diamondite data this is not feasible as the absolute elemental concentrations mainly reflect the (highly variable) abundance of microinclusions (fluid±solid) in the samples. Hence only the changes in trace-element ratios (element fractionation) can be used to track the evolution of the diamond-forming fluids during diamond crystallisation. Table 4 shows the ratios (chondrite-normalised for comparison with bulk-earth values) of some of the key trace-element ratios, such as the HFSE (e.g. Zr/Hf, Nb/Ta), and the Sr, Y and Yb anomalies for the diamondites and some of the inferred phases. Their trace-element ratios can be compared to the diamondites to test whether the crystallisation of such phases can explain the trace-element data or whether another mechanism is responsible for the observed patterns.

The average Zr/Hf is chondritic in both the P and E diamondites, suggesting that no fractionation occurred between these two elements during crystallisation. The mineral phases whose presence is inferred above (garnet, clinopyroxene, LIMA, ilmenite, mica) all have chondritic or near-chondritic ratios and hence their crystallisation would not be expected to change the Zr/Hf ratio.

Nb/Ta shows a larger range, varying from 0.005 to 11.4; the "peridotitic" diamondites have Nb/Ta of 0.005 to 2.19, whereas the "eclogitic" diamondites vary from 0.1 to 11.4. Ilmenite, LIMA and garnet (as found in D017) all have sub-chondritic Nb/Ta, and their crystallisation would tend to raise Nb/Ta in the residual fluid, while crystallisation of clinopyroxene (or garnet – as found in D012) (Nb/Ta≥1) could shift the ratio towards lower values. The observed scatter in Nb/Ta may be due to the competing effects of the crystallisation of these phases.

Nb/Zr is also quite variable in both parageneses, with most "eclogitic" samples falling between 0.13 and 52.4, and the peridotitic diamondites between 1.3 and 98.1. Crystallisation of garnet will drive Nb/Zr up in the residual fluid, while crystallisation of ilmenite and mica will drive it downwards.

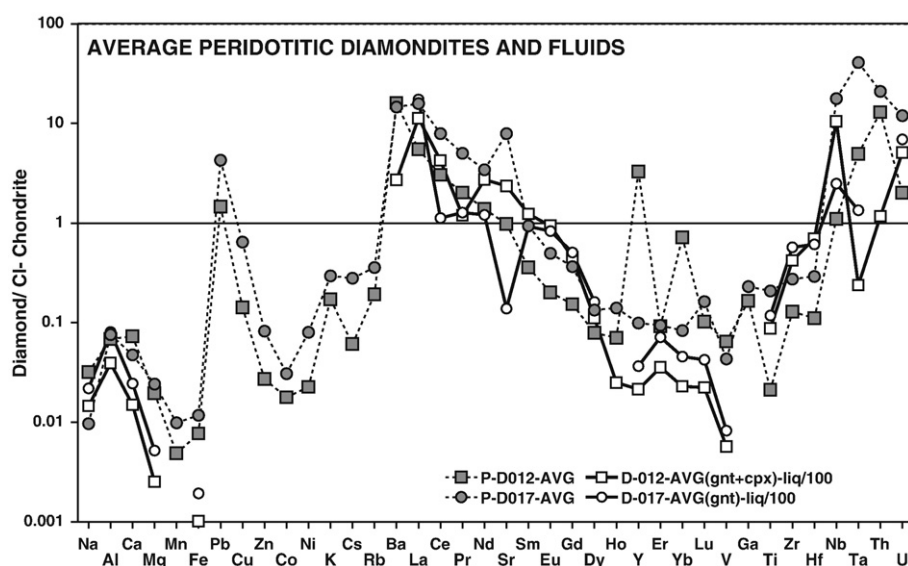


**Fig. 3.** Chondrite-normalised trace-element patterns for peridotitic diamondites DIA-012 and DIA-017 (solid symbols), compared with the compositions of coexisting fluids calculated from the trace-element compositions of garnet and clinopyroxene (open symbols).

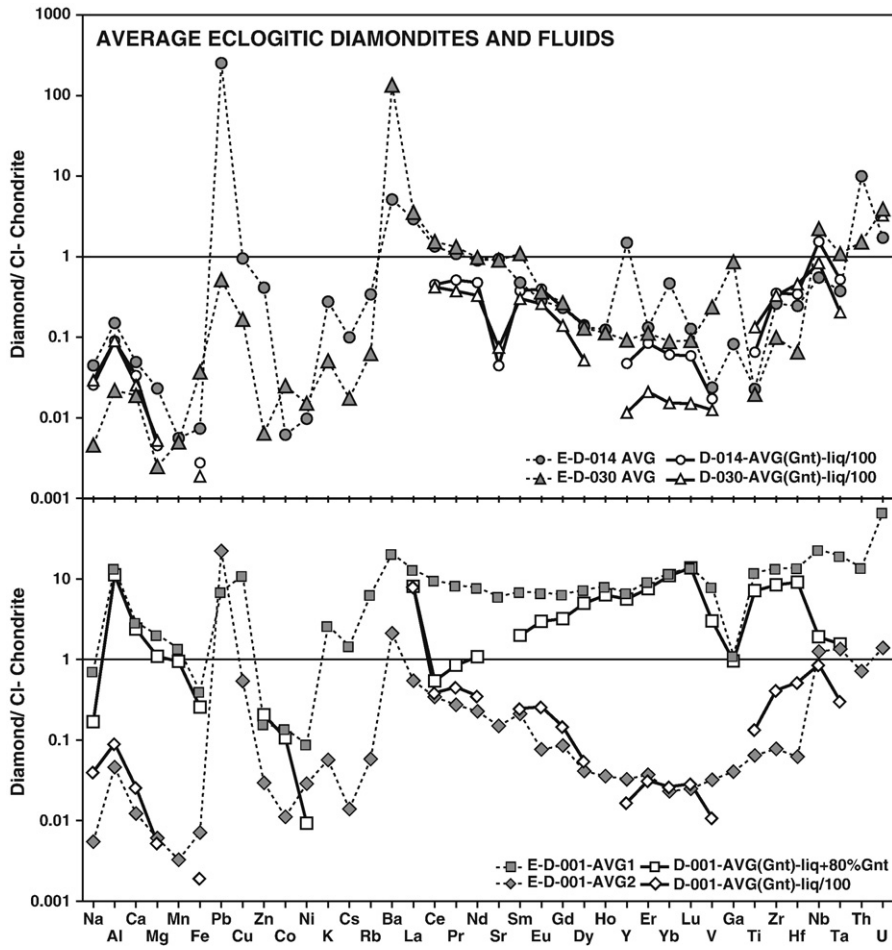


**Fig. 4.** Chondrite-normalised trace-element patterns for eclogitic diamondites DIA-001, DIA-014 and DIA-030 (solid symbols), compared with the compositions of coexisting fluids calculated from the trace-element compositions of garnet (open symbols).

Therefore, the variations in Nb/Ta and Nb/Zr, and the lack of Zr/Hf fractionation between the P-type and E-type diamondites, are consistent with the crystallisation of ilmenite, garnet and clinopyroxene from the fluid. As the Zr/Hf of ilmenite is around 0.5, and its Nb/Ta is ~0.4, the removal of ilmenite from the fluid does not produce a large effect on the Zr/Hf or Nb/Ta of the diamondite.

The Th/U values of the diamondites show considerable scatter, ranging from ~0.1 to 30. The fractionation of Th and U could be explained by the crystallisation of clinopyroxene from the fluid. The Th/U of clinopyroxene intergrown with the diamondites (Dobosi and Kurat, 2002) is ~0.25. The crystallisation of small amounts of phases such as apatite (e.g. O'Reilly and Griffin, 2000) or LIMA (authors' unpublished data) that have high Th and U contents (and low Th/U) could cause a rapid rise in the ratio, possibly producing the observed scatter.

The difference in the Cr contents of the P and E garnets may be explained by the crystallisation of chromite, as suggested by Dobosi and Kurat (2002). Removal of chromite will not affect the REE and will have minimal effect on the HFSE, as they are not abundant in chromite. As noted above, this hypothesis could not be tested by the methods used here.

A wide range in Ni and Co contents in the diamondites (Table 4) suggests that a sulfide phase was crystallizing from the fluid (or a sulfide liquid was separating) as diamond was precipitating. There is a weak positive correlation between Mg and Ni, and a better correlation between Cu and Ni (Fig. 5) and Fe and Ni (not shown). The absence of olivine as an inclusion phase in the diamondites (Kurat and Dobosi, 2000; Dobosi and Kurat 2002), and the correlations mentioned above,

suggest sulfide as a major host for Ni and Co, as well as Cu. However, crystallisation of mica, LIMA or clinopyroxene may also have contributed to the weak positive correlation between Mg and Ni (Fig. 5).

The Y/Yb for most analyses of both the P and E diamondites is chondritic although a few analyses have a higher ratio (up to 19.7, Table 4). Many of the analyses show a positive Y anomaly, accompanied in some cases by an Yb anomaly (Fig. 6). These patterns may reflect the 'contamination' of the analysis by solid phases such as fluorite ( $Y/Yb \sim 11$ ) and/or fluorapatite ( $Y/Yb \sim 2.25$ ) from carbonatites, which have REE patterns with positive Y anomalies (Bühn et al., 2001, 2002) and/or LIMA with positive Yb anomalies (authors' unpublished data). The crystallisation of these phases would leave the fluid with large negative Y and Yb anomalies, and the chondritic Y/Yb observed in most of the diamondite analyses suggests that these phases only crystallised locally.

#### 5.4. Comparison of "peridotitic" and "eclogitic" diamondites

Fig. 7 shows the average trace-element pattern for each diamondite sample. With the exception of two samples (peridotitic diamondite Dia-078, which may be carbonate-rich, and "eclogitic" diamondite Dia-001, which is garnet-rich) the two sets of patterns are similar, though detailed comparison reveals subtle differences. The diamondite data therefore support the conclusions of Dobosi and Kurat (2002), who suggested that the compositional similarity of the "peridotitic" and "eclogitic" garnets in the diamondites, which differ mainly in their Cr contents, reflects similarities in the fluids or melts from which they

**Table 3**

Average hypothetical liquid concentrations compared with average diamondite values (chondrite-normalised)

Element	Peridotitic diamondites				Eclogitic diamondites							
	D-012		D-017		D-001		D-014		D-030			
	AVG(Gnt+Cpx)-liq/100	P-D012-AVG	AVG(Gnt+Cpx)-liq/100	P-D017-AVG	AVG(Gnt)-liq/100	AVG(Gnt)-liq + 80%Gnt	E-D-001-AVG1	E-D-001-AVG2	AVG(Gnt)-liq/100	E-D-014-AVG	AVG(Gnt)-liq/100	E-D-030-AVG
Na	0.01	0.03	0.02	0.01	0.04	0.17	0.72	0.01	0.03	0.04	0.03	0.005
Al	0.04	0.07	0.08	0.08	0.09	11.2	13.5	0.05	0.09	0.15	0.09	0.02
Ca	0.01	0.07	0.02	0.05	0.03	2.37	2.89	0.01	0.03	0.05	0.03	0.02
Mg	0.003	0.02	0.01	0.02	0.01	1.10	2.03	0.01	0.004	0.02	0.01	0.002
Mn	0	0.005	0	0.01	0	0.94	1.37	0.003	0	0.006	0	0.005
Fe	0.001	0.008	0.002	0.01	0.002	0.26	0.40	0.007	0.003	0.007	0.002	0.04
Pb	0	1.45	0	4.25	0	0	6.90	22.2	0	252	0	0.51
Cu	0	0.14	0	0.64	0	0	11.0	0.54	0	0.94	0	0.17
Zn	0	0.03	0	0.08	0	0.20	0.16	0.03	0	0.41	0	0.01
Co	0	0.02	0	0.03	0	0.11	0.14	0.01	0	0.01	0	0.02
Ni	0	0.02	0	0.08	0	0.01	0.09	0.03	0	0.01	0	0.02
K	0	0.17	0	0.29	0	0	2.62	0.06	0	0.28	0	0.05
Cs	0	0.06	0	0.28	0	0	1.47	0.01	0	0.10	0	0.02
Rb	0	0.19	0	0.36	0	0	6.36	0.06	0	0.34	0	0.06
Ba	2.70	16.0	0	14.6	0	0	20.6	2.11	0	5.10	0	134
La	11.2	5.49	17.3	15.8	8.02	8.08	13.0	0.54	0	2.90	0	3.53
Ce	4.25	3.03	1.12	7.86	0.38	0.54	9.61	0.34	0.45	1.34	0.42	1.53
Pr	1.19	2.01	1.27	5.02	0.45	0.85	8.34	0.27	0.51	1.08	0.37	1.32
Nd	2.72	1.39	1.21	3.41	0.35	1.07	7.77	0.23	0.47	0.90	0.33	0.97
Sr	2.34	0.97	0.14	7.89	0	0	6.05	0.15	0.04	0.93	0.07	0.90
Sm	1.23	0.36	0.92	0.94	0.25	1.98	6.92	0.21	0.38	0.48	0.30	1.09
Eu	0.94	0.20	0.83	0.49	0.26	2.96	6.68	0.08	0.39	0.28	0.26	0.36
Gd	0.45	0.15	0.50	0.36	0.15	3.20	6.45	0.09	0.23	0.23	0.14	0.27
Dy	0.11	0.08	0.16	0.13	0.05	4.93	7.31	0.04	0.14	0.13	0.05	0.13
Ho	0.02	0.07	0	0.14	0	6.30	8.02	0.04	0	0.12	0	0.11
Y	0.02	3.26	0.04	0.10	0.02	5.62	6.67	0.03	0.05	1.49	0.01	0.09
Er	0.04	0.09	0.07	0.09	0.03	7.53	9.24	0.04	0.08	0.13	0.02	0.11
Yb	0.02	0.71	0.05	0.08	0.03	11.0	11.6	0.02	0.06	0.46	0.02	0.09
Lu	0.02	0.10	0.04	0.16	0.03	13.7	13.8	0.02	0.06	0.13	0.01	0.09
V	0.006	0.06	0.01	0.04	0.01	3.01	7.94	0.03	0.02	0.02	0.01	0.24
Ga	0	0.16	0	0.23	0	0.96	1.11	0.04	0	0.08	0	0.86
Ti	0.09	0.02	0.12	0.21	0.13	7.11	11.9	0.06	0.06	0.02	0.13	0.02
Zr	0.42	0.13	0.57	0.27	0.41	8.37	13.4	0.08	0.35	0.26	0.33	0.10
Hf	0.69	0.11	0.61	0.29	0.52	9.06	13.7	0.06	0.34	0.24	0.45	0.07
Nb	10.4	1.10	2.47	17.7	0.86	1.89	23.1	1.25	1.53	0.55	0.83	2.21
Ta	0.24	4.94	1.34	40.7	0.30	1.54	19.3	1.35	0.52	0.37	0.20	1.09
Th	1.17	13.0	0	20.9	0	0	13.8	0.71	0	9.93	0	1.51
U	5.05	2.01	6.89	11.9	0	0	66.8	1.39	0	1.71	3.22	3.88

precipitated. They suggested that the fluids evolved from “peridotitic” to “eclogitic” through the subtraction of chromite; the analyses presented here support that conclusion.

The “peridotitic” diamondites on average have small positive anomalies in Sr, Y and Yb, which are not as pronounced in the “eclogitic” diamondites. The “eclogitic” diamondites have generally

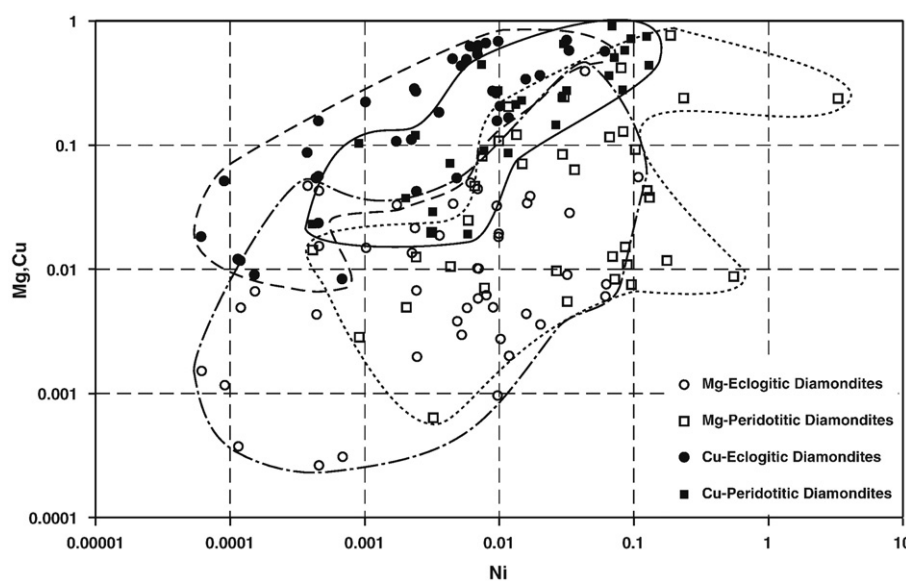


**Fig. 5.** Plot of Mg vs Ni (chondrite-normalised) and Cu vs Ni for peridotitic and eclogitic diamondites showing broad positive correlations among these elements.

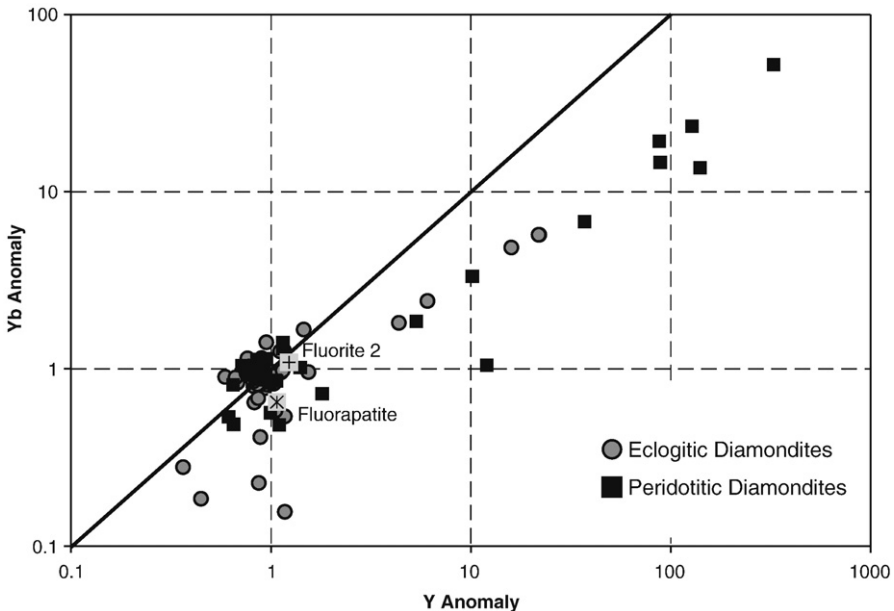


**Fig. 6.** Plot of Y anomaly vs Yb anomaly (chondrite-normalised) for peridotitic and eclogitic diamondites, illustrating the covariation of Y and Yb ascribed to the presence of a postulated fluoride phase.

higher Nb/Ta than the “peridotitic” diamondites (average Nb/Ta ranges from 0.70 to 2.47 for the E-type and 0.22 to 0.99 for the P-type) but a similar range of Th/U (Th/U of E-type=0.21 to 7.29, P-type=0.45 to 6.46). The “eclogitic” diamondites also have lower abundances of Cr, Mn, Co and Ni than the “peridotitic” diamondites. These differences suggest that sulfide and ilmenite (and possibly carbonates) have been removed from the fluid along with chromite during evolution from the “peridotitic” diamondites to the “eclogitic” diamondites. The small differences between the eclogitic and peridotitic diamondites are reflected in the similarity of the calculated parental fluids (Fig. 8); the main difference is in the lower LREE/HREE of the eclogitic fluids which might reflect the crystallisation of clinopyroxene.

An analogy to this fluid evolution may be provided by the analyses of two mantle-derived garnet megacrysts with coexisting red and orange garnets, recovered from the Kaalvallei kimberlite, South Africa (Moore and Belousova, 2005). In these samples, the orange garnet (Cr-poor) encloses or partially encloses a red garnet (Cr-rich), which in turn contains inclusions of olivine, orthopyroxene and clinopyroxene. The interface between the two garnet varieties is marked by a necklace of small irregular ilmenite blebs. This assemblage may represent a transitional stage between the “peridotitic” and “eclogitic” growth environments and the presence of ilmenite supports the suggestion that it crystallises during this transition.

### 5.5. Origin of the parental fluids

Fig. 9 compares the diamondite patterns to those of an average kimberlite (Mitchell, 1986) and an average carbonatite (Woolley and Kempe, 1989); carbonatite melt inclusions, derived from depths of ca 180 km below the Slave Craton, have similar patterns (van Achterbergh et al., 2002, 2004). The REE and HFSE patterns for the diamondites, the carbonatite and the kimberlite are all very similar. There are minor differences in the ‘major’ elements; the diamondite patterns show higher Na and Al relative to Ca than either carbonatite or kimberlite. The chalcophile elements (Pb to Ni) also are higher in most diamondites, relative to Fe or Mg. However, the overall similarity of the patterns for the analysed diamondites, the kimberlite and the carbonatite suggests that the diamondites have crystallized from a fluid in the kimberlite–carbonatite spectrum, as previously suggested

by Gurney and Boyd (1982; Jwaneng framesite) and Dobosi and Kurat (2002; these samples). The various other phases whose presence is inferred from this study (carbonate, sulfide, fluorite, mica, LIMA) can account for the sample-to-sample variation in the relative abundances of specific trace elements.

The trace-element data obtained from this study do not allow a distinction between a kimberlitic or carbonatitic affinity for the parental fluid. Jacob et al. (2000) suggested a carbonatitic origin for the framesites from Venetia, based in part on variations in the Sr contents in garnets of eclogitic affinity found in the framesites. In the Venetia samples, Sr is locally enriched by up to a factor of 19 and is accompanied by enrichment in LREE; these variations cannot be attributed to core-rim zoning. Core-rim zonation of Sr also was observed in a peridotitic diamond-inclusion garnet reported by Shimizu and Sobolev (1995), who interpreted the zoning as the result of rapid growth in a fractionating melt. The preservation of trace-element zonation implies that the framesites (and the monocrystalline diamond studied by Shimizu and Sobolev, 1995) were entrained in the kimberlite shortly after their crystallisation. However, based on the more radiogenic  $^{87}\text{Sr}/^{86}\text{Sr}$  signature and much higher Sr contents of the host kimberlite compared with the framesite, Jacob et al. (2000) concluded that the framesites are genetically unrelated to the host kimberlite.

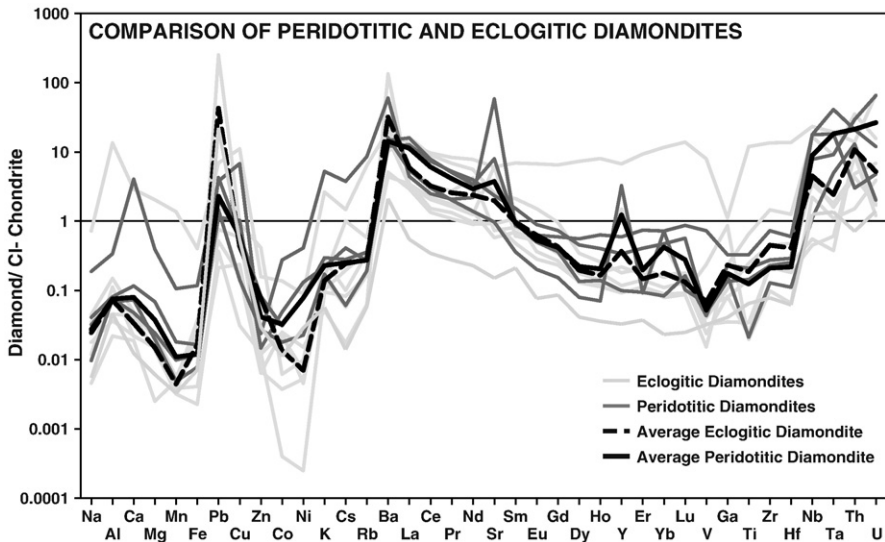
Litvin et al. (2005) have demonstrated the crystallisation of diamondite, grossular-almandine garnet and diopside from a natural carbonatite composition at 7.0–8.5 GPa and 1800 °C; diamondite crystallised very rapidly from the C-enriched carbonate–silicate melt. Although the experimental P and T probably are much higher than those in which natural diamondites form, these studies demonstrate the feasibility of a carbonatite-related origin for the diamondites.

Fig. 10 compares the average trace-element patterns of the diamondites with the trace-element patterns for a fibrous diamond from Jwaneng, previously analysed by this technique (Rege et al., 2005). The patterns for these two diamond types are remarkably similar although the overall levels of impurities are higher in the diamondites.

From the above observations it can be suggested that both “peridotitic” and “eclogitic” diamondites, and fibrous diamonds such as those from Jwaneng, have grown from a ‘silico-carbonatitic’ fluid/

**Table 4**  
Chondrite-normalised element ratios in diamondites and possible minor phases

	Sample	Th/U			Nb/Ta			Zr/Hf			Co/Ni			Y anomaly			Nb/Zr			Y/Yb			
		MAX	MIN	AVG	MAX	MIN	AVG	MAX	MIN	AVG	MAX	MIN	AVG	MAX	MIN	AVG	MAX	MIN	AVG	MAX	MIN	AVG	
This study	Peridotitic diamondites																						
	D-012	29.8	1.40	6.46	1.567	0.005	0.221	2.287	0.557	1.162	2.52	0.309	0.788	319.1	0.969	40.32	24.07	1.309	8.522	10.69	1.30	4.571	
	D-017	5.45	0.66	1.75	1.052	0.128	0.433	1.447	0.316	0.940	0.581	0.351	0.385	1.763	0.634	0.845	98.08	5.759	64.60	1.80	0.755	1.185	
	D-054	5.97	0.09	0.45	2.191	0.234	0.857	2.237	0.269	0.90	1.078	0.286	0.373	0.918	0.60	0.833	89.91	8.70	34.36	1.127	0.53	0.716	
	D-078	1.26	0.15	0.63	1.938	0.874	0.985	1.668	1.044	1.214	0.985	0.40	0.669	1.029	0.70	0.865	31.76	13.43	24.56	1.180	0.50	0.828	
	Eclogitic diamondites																						
	D-001	1.26	0.12	0.21	1.82	0.72	1.18	2.27	0.73	0.98	3.68	0.36	1.34	1.14	0.74	0.77	20.9	0.80	1.78	1.84	0.52	0.58	
	D-014	14.5	2.04	5.82	7.62	0.70	1.46	1.65	0.87	1.06	0.92	0.55	0.63	21.3	1.09	11.7	5.14	0.99	2.1	3.62	1.36	3.21	
	D-022	7.05	0.38	2.26	11.4	0.10	1.83	1.70	0.86	1.16	2.23	0.86	1.61	1.17	0.43	0.73	52.4	0.13	11.4	19.7	0.81	1.18	
	D-030	1.42	0.23	0.39	4.53	1.12	2.03	4.45	1.17	1.51	3.32	1.21	1.65	1.41	0.70	0.82	37.0	8.84	22.5	5.06	0.95	1.04	
	D-052	14.1	2.31	7.29	1.65	0.20	0.74	1.34	1.00	1.20	1.88	0.62	0.71	1.49	0.79	1.23	3.35	1.15	2.07	2.49	0.70	1.28	
	D-053	1.26	0.29	0.70	3.78	0.58	1.90	1.29	0.80	0.96	17.4	3.57	5.44	0.92	0.64	0.73	16.5	2.09	7.51	1.77	0.71	1.07	
	D-057	6.07	0.83	2.38	3.77	0.88	2.47	1.26	0.59	0.94	3.55	2.76	3.08	0.86	0.35	0.77	26.6	1.17	18.0	3.22	0.73	1.15	
Dobosi and Kurat (2002)	Clinopyroxene-D012	0.24			1.00			0.54			1.27			0.92			0.56			2.00			
	Garnet-D012	–			1.34			1.67			14.9			0.88			0.47			0.73			
	Garnet-D017	–			0.54			1.08			8.40			0.77			0.27			0.64			
Griffin (unpublished data)	LIMA	0.03			0.47			0.77			4.04			0.77			3.54			0.24			
Deines and Harris (1995)	Sulphide–Orapa	–			–			–			1.22			–			–			–			
Griffin et al. (1997)	Ilmenite–Orapa	–			0.41			0.58			5.44			–			33.6			–			
O'Reilly and Griffin (2000)	Carbonate–Apatite/100	0.62			–			–			–			1.11			1.62			2.01			
van Achterbergh (2004)	Mica (Phlogopite)	0.25			0.71			0.66			0.77			3.97			35.0			7.85			
S. Jackson pers. comm., 2005	Fluorite-1	–			–			–			–			5.31			–			11.3			
Bühn et al. (2002)	Fluorite-2	1.47			–			–			–			1.24			–			1.17			
Bühn et al. (2001)	Fluorapatite	–			–			–			–			1.07			–			2.25			
van Achterbergh (2004)	Carbonate Bleb	0.02			0.42			2.82			5.15			0.46			0.60			0.17			
van Achterbergh (2004)	Silicate Bleb	–			–			–			–			–			46.8			–			



**Fig. 7.** Comparison of average chondrite-normalised trace-element patterns for peridotitic and eclogitic diamondites. Light lines show average patterns for individual samples; heavy solid and dashed lines show overall averages for each type.

melt in the kimberlite–carbonatite spectrum (Dalton and Presnall, 1998). This melt apparently had a large carbonate component and was able to crystallise other associated phases (garnet, clinopyroxene, sulfide, fluoride, mica, ilmenite, LIMA).

## 6. Conclusions

- “Peridotitic” and “eclogitic” diamondites have probably crystallised from the same type of fluid, which evolved by the removal of chromite±sulfide±ilmenite.
- This parental fluid had a trace-element and major-element pattern similar to an average carbonatite and/or kimberlite, and is similar to the fluids that produced some fibrous diamonds.
- The presence of various (micron-sized?) solid phases, in addition to macroscopic garnet and clinopyroxene, can be inferred from the diamondite trace-element data. These phases are: a Y-Yb rich (fluoride?) phase, a Cu-Pb-Zn-Co-Ni sulfide phase, a LIMA-type

phase, a carbonate, an ilmenite-like phase, chromite and mica. Crystallisation of these phases may have controlled the trace-element composition of the fluid during diamondite crystallisation.

## Acknowledgements

This work has been made possible by the dedicated help and guidance provided by the staff of the GEMOC Geochemical Analysis Unit: Suzy Elhlou, Peter Weiland, Tin Tin Win and Carol Lawson. We thank Chris Tye and Fred Fryer (Agilent Technologies) for advice on analytical problems. A detailed constructive review by the two anonymous referees and by Claude Dalpé helped to improve the MS. Financial support from Macquarie University has included an IPRS scholarship and a grant from the Postgraduate Research Fund (S. Rege). Much of the analytical work was supported through an ARC Discovery Project grant (SYO'R and WLG), and used instrumentation funded by ARC LIEF and DEST Systemic Infrastructure Grants,

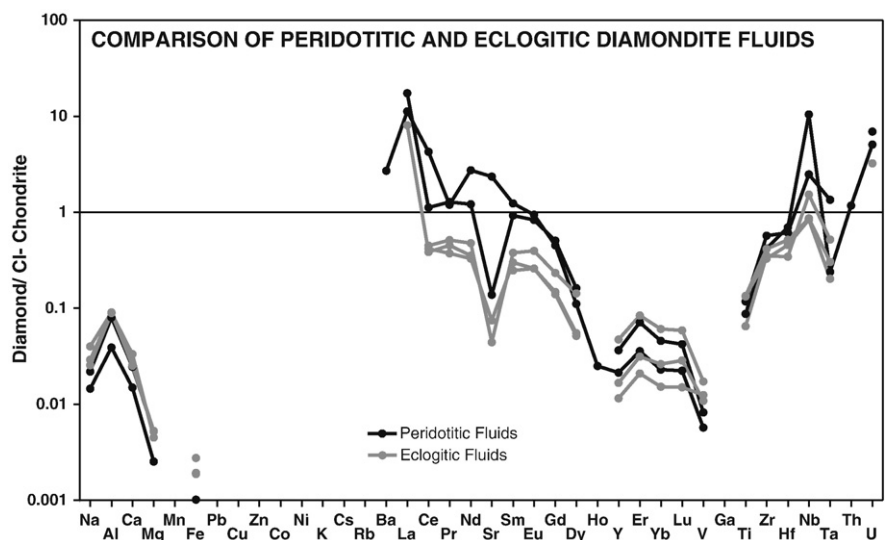


**Fig. 8.** Comparison of fluids coexisting with garnet±clinopyroxene in peridotitic and eclogitic diamondites, calculated using inclusion trace-element data from Dobosi and Kurat (2002) and partition coefficients given in Table 2.

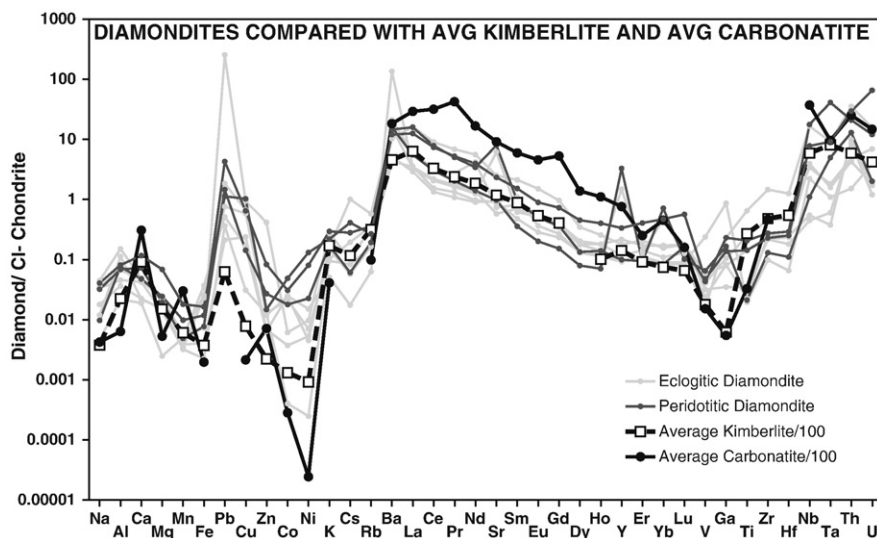


**Fig. 9.** Comparison of average chondrite-normalised trace-element patterns of peridotitic and eclogitic diamondites with the patterns of average kimberlite and carbonatite (divided by 100 for better comparison).

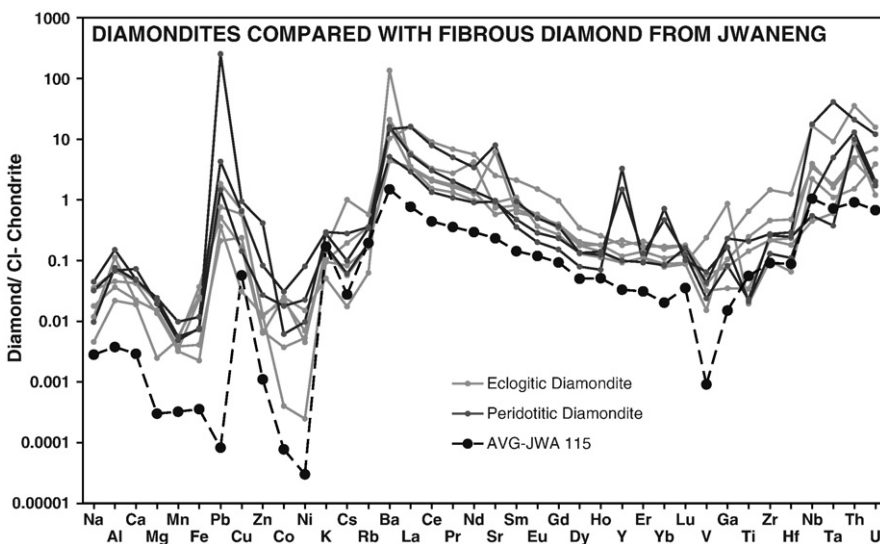


**Fig. 10.** Comparison of the average chondrite-normalised trace-element patterns of diamondites (peridotitic and eclogitic) with the pattern of a typical fibrous diamond from Jwaneng (data from Rege et al., 2005).

Macquarie University and Industry. This is contribution no. 540 from the ARC National Key Centre for the Geochemical Evolution and Metallogeny of Continents ([www.els.mq.edu.au/GEMOC/](http://www.els.mq.edu.au/GEMOC/)).

#### Appendix A. Supplementary data

Supplementary data associated with this article can be found, in the online version, at [doi:10.1016/j.lithos.2008.06.002](https://doi.org/10.1016/j.lithos.2008.06.002).

#### References

- Bulanova, G.P., Pavlova, L.P., 1987. Magnesite peridotite assemblage in diamond from the Mir pipe. *Doklady Akademii nauk SSSR* 295 (6), 1452–1456.
- Bühn, B., Rankin, A.H., 1999. Composition of natural, volatile-rich Na–Ca–REE–Sr carbonatitic fluids trapped in fluid inclusions. *Geochimica et Cosmochimica Acta* 63, 3781–3797.
- Bühn, B., Wall, F., Le Bas, M.J., 2001. Rare-earth element systematics of carbonatitic fluorapatites, and their significance for carbonatitic magma evolution. *Contributions to Mineralogy and Petrology*, 141, 572–591.
- Bühn, B., Rankin, A.H., Schneider, J., Dulski, P., 2002. The nature of orthomagmatic, carbonatitic fluids precipitating REE, Sr-rich fluorite: fluid-inclusion evidence from the Okorusu fluorite deposit, Namibia. *Chemical Geology* 186, 75–98.
- Dalton, J.A., Presnall, D.C., 1998. The continuum of primary carbonatitic–kimberlitic melt compositions in equilibrium with lherzolite: data from the system CaO–MgO–Al<sub>2</sub>O<sub>3</sub>–SiO<sub>2</sub>–CO<sub>2</sub> at 6 GPa. *Journal of Petrology* 39, 1953–1964.
- Davies, R., Griffin, W.L., Pearson, N.J., Andrew, A.S., Doyle, B.J., O'Reilly, S.Y., 1999. Diamonds from the Deep: Pipe D0-27, Slave Craton, Canada, Extended Abstracts, 7th International Kimberlite Conference, Cape Town, pp. 170–172.
- Deines, P., Harris, J.W., 1995. Sulfide inclusion chemistry and carbon isotopes of African diamonds. *Geochimica et Cosmochimica Acta* 59 (15), 3173–3188.
- Dobosi, G., Kurat, G., 2002. Trace element abundances in garnets and clinopyroxenes from diamondites; a signature of carbonatitic fluids. *Mineralogy and Petrology* 76 (1–2), 21–38.
- Fujimaki, H., Tatsumoto, M., Aoki, K., 1984. Partition coefficients of Hf, Zr, and REE between phenocrysts and groundmasses. *Journal of Geophysical Research* 89, B662–B672 Suppl.
- Griffin, W.L., Moore, R.O., Ryan, C.G., Gurney, J.J., Win, T.T., 1997. Geochemistry of magnesian ilmenite megacrysts from southern African kimberlites. *Proc. 6th Int. Kimb. Conf. Geology and Geophysics*, vol. 38(2), pp. 421–443.
- Gurney, J.J., Boyd, F.R., 1982. Mineral intergrowths with polycrystalline diamonds from the Orapa Mine, Botswana. *Year Book – Carnegie Institution of Washington* 82, 267–273.
- Guthrie, G.D., Veblen, D.R., Navon, O., Rossman, G.R., 1991. Submicrometer fluid inclusions in turbid-diamond coats. *Earth and Planetary Science Letters* 105 (1–3), 1–12.
- Haggerty, S.E., 1983. The mineral chemistry of new titanates from the Jagersfontein kimberlite, South Africa: implications for metasomatism in the upper mantle. *Geochimica et Cosmochimica Acta* 47, 1833–1854.

- Haggerty, S.E., 1987. Metasomatic mineral titanates in upper mantle xenoliths. In: Nixon, P.H. (Ed.), *Mantle Xenoliths*. Wiley, Chichester, pp. 671–690.
- Harris, J.W., 1992. Diamond geology. In: Field, J.E. (Ed.), *The Properties of Natural and Synthetic Diamond*. Academic Press, London, pp. 343–393.
- Hauri, E.H., Wagner, T.P., Grove, T.L., 1994. Experimental and natural partitioning of Th, U, Pb and other trace elements between garnet, clinopyroxene and basaltic melts. *Chemical Geology* 117 (1–4), 149–166.
- Honda, M., Phillips, D., Harris, J.W., Yatsevich, I., 2004. Unusual noble gas compositions in polycrystalline diamonds: preliminary results from the Jwaneng Kimberlite, Botswana. *Chemical Geology* 203 (3–4), 347–358.
- Izraeli, E.S., Harris, J.W., Navon, O., 2004. Fluid and mineral inclusions in cloudy diamonds from Koffiefontein, South Africa. *Geochimica et Cosmochimica Acta* 68, 2561–2575.
- Jacob, D.E., Viljoen, K.S., Grassineau, N., Jagoutz, E., 2000. Remobilization in the cratonic lithosphere recorded in polycrystalline diamond. *Science* 289 (5482), 1182–1185.
- Jacob, D.E., Kronz, A., Viljoen, K.S., 2004. Cohenite, native iron and troilite inclusions in garnets from polycrystalline diamond aggregates. *Contributions to Mineralogy and Petrology* 146 (5), 566–576.
- Jenner, G.A., Foley, S.F., Jackson, S.E., Green, T.H., Fryer, B.J., Longerich, H.P., 1993. Determination of partition coefficients for trace elements in high pressure-temperature experimental run products by laser ablation microprobe-inductively coupled plasma-mass spectrometry (LAM-ICP-MS). *Geochimica et Cosmochimica Acta* 57 (23–24), 5099–5103.
- Kirkley, M.B., Gurney, J.J., Rickard, R.S., 1994. Jwaneng framesites: carbon isotopes and intergrowth compositions. In: Meyer, H.O.A., Leonards, O.H. (Eds.), *Diamonds: Characterisation, Genesis and Exploration*, vol. 1/B. CPRM Special Publ., pp. 127–135.
- Klemme, S., 2004. Evidence for fluoride melts in the Earth's mantle formed by liquid immiscibility. *Geology* 32 (5), 441–444.
- Kurat, G., Dobosi, G., 2000. Garnet and diopside-bearing diamondites (framesites). *Mineralogy and Petrology* 69 (3–4), 143–159.
- Leung, I.S., 1984. The discovery of calcite inclusion in natural diamond and its implications on the genesis of diamond, kimberlite and carbonatite. Geological Society of America, Abstracts with Programs 16, 574.
- Leung, I.S., 1990. Silicon carbide cluster entrapped in a diamond from Fuxian, China. *American Mineralogist* 75, 1110–1119.
- Litvin, Y.A., Kurat, G., Dobosi, G., 2005. Experimental study of diamondite formation in carbonate-silicate melts: a model approach to natural processes. *Russian Geology and Geophysics* 46, 1304–1317.
- McDade, P., Harris, J.W., 1999. Syngenetic inclusion bearing diamonds from Letseng-la-Terai, Lesotho. In: Gurney, J.J., Gurney, J.L., Pascoe, M.D., Richardson, S.H. (Eds.), *7th International Kimberlite Conference*, Cape Town, pp. 557–565.
- McDonough, W.F., Sun, S.-S., 1995. The composition of the Earth. *Chemical Geology* 120, 223–253.
- Meyer, H., 1987. Inclusions in diamond. In: Nixon, P.H. (Ed.), *Mantle Xenoliths*. J Wiley & Sons, Chichester, pp. 501–522.
- Mitchell, R.H., 1986. *Kimberlites*. Plenum Press, New York. 442 pp.
- Moore, A., Belousova, E., 2005. Crystallization of the Cr-poor and Cr-rich megacryst suites from the same (host kimberlite) magma. *Contributions to Mineralogy and Petrology* 149, 462–481.
- Nixon, P.H., 1987. *Mantle Xenoliths*. John Wiley and Sons. 864 pp.
- O'Reilly, S.Y., Griffin, W.L., 2000. Apatite in the mantle: implications for metasomatic processes and high heat production in Phanerozoic mantle. *Lithos* 53, 217–232.
- Orlov, Y.L., 1977. *The Mineralogy of the Diamond*. Wiley, New York. 342 pp.
- Rege, S., Jackson, S., Griffin, W.L., Davies, R.M., Pearson, N.J., O'Reilly, S.Y., 2005. Quantitative trace-element analysis of diamond by laser ablation inductively coupled plasma mass spectrometry. *Journal of Atomic Analytical Spectrometry* 20 (7), 601–611.
- Schrauder, M., Navon, O., 1993. Solid carbon-dioxide in a natural diamond. *Nature* 365 (6441), 42–44.
- Shimizu, N., Sobolev, N.V., 1995. Young peridotitic diamonds from the Mir kimberlite pipe. *Nature*, 375 (6530), 394–397.
- van Achterbergh, E., Ryan, C., Jackson, S., Griffin, W., 2001. Appendix 3 data reduction software for LA-ICP-MS in laser-ablation-ICPMS in the Earth Sciences. In: Sylvester, P. (Ed.), *Mineralogical Association of Canada Short Course*, vol. 29, pp. 239–243.
- van Achterbergh, E., Griffin, W.L., O'Reilly, S.Y., Ryan, C.G., Pearson, N.J., Kivi, K., Doyle, B.J., 2004. Melt inclusions from the deep slave lithosphere: implications for the origin and evolution of mantle-derived carbonatite and kimberlite. *Lithos* 76, 461–474.
- van Achterbergh, E., Griffin, W.L., Ryan, C.G., O'Reilly, S.Y., Pearson, N.J., Kivi, K., Doyle, B.J., 2002. Subduction signature for quenched carbonatites from the deep lithosphere. *Geology* 30 (8), 743–746.
- Walmsley, J.C., Lang, A.R., 1992. On submicrometer inclusions in diamond coat – crystallography and composition of ankerites and related rhombohedral carbonates. *Mineralogical Magazine* 56 (385), 533–543.
- Wang, A., Pasteris, J.D., Meyer, H.O.A., DeleDuboï, M.L., 1996. Magnesite-bearing inclusion assemblage in natural diamond. *Earth and Planetary Science Letters* 141 (1–4), 293–306.
- Woolley, A.R., Kempe, D.R.C., 1989. Carbonatites: nomenclature, average chemical compositions and element distribution. In: Bell, K. (Ed.), *Carbonatites: Genesis and Evolution*, pp. 1–14.
- Zhou, J., Yang, G., Zhang, J., 1984. Mathiasite in a kimberlite from China. *Acta Mineral. Sinica* 9, 193–200.